# MAGNETIC CONTINUOUSLY VARIABLE TRANSMISSION FOR REDUCTION OF WIND TURBINE DRIVETRAIN SIZE

An Undergraduate Research Scholars Thesis

by

ELLEN DANGTRAN

Submitted to the Undergraduate Research Scholars program at
Texas A&M University
in partial fulfillment of the requirements for the designation as an

UNDERGRADUATE RESEARCH SCHOLAR

Approved by Research Advisor: Dr. Hamid Toliyat

May 2019

Major: Electrical Engineering

# TABLE OF CONTENTS

# ABSTRACT

Magnetic Continuously Variable Transmission for Reduction of Wind Turbine Drivetrain Size

Ellen Dangtran
Department of Electrical Engineering
Texas A&M University

Research Advisor: Dr. Hamid Toliyat
Department of Electrical Engineering
Texas A&M University

The objective of this research is to do analysis on magnetic gears for the application of Magnetic Continuously Variable Transmissions (mCVTs) on wind turbines. Wind turbines convert the kinetic energy of wind into electrical energy. A primary component of the wind turbine is the gearbox. Currently, mechanical gears are used in the gearbox; however, there are several issues with the physical contact required to transfer power between the shafts, such as wear-and-tear, heat, and misalignment.

Magnetic gears are a potential solution to many of these problems as they function without contact and are not as severely impacted by misalignment. Bidirectional conversion for the control rotor, harnessing wind at all possible wind speeds, and increasing speed while holding torque, are all desirable features of an mCVT for wind turbines; however, they each require a larger and more expensive power electronics converter in the drivetrain.

A two-axis testbed and a magnetic gear prototype is designed to test the impact of misalignment on the operation of the magnetic gear. Solutions to reducing the size and cost of the power electronics considered in this research include: only using unidirectional converters on the control rotor, using optimum gear ratios, considering different synchronous generator speeds, and

only harnessing wind above certain wind speeds. Matlab data is collected to compare wind speed to the output power, analyze power generation capacity lost by using only a unidirectional, and review power to gear ratio relationships. The costs and benefits of each solution is considered based on the data collected.

The experimental data from the prototype is compared to simulated data on the prototype to compare the evaluate the demonstrator. The data from the prototype is used to form torque angle curves of the magnetic gears at varying misalignments and is evidence that the magnetic gear is a viable replacement for mechanical gears.

# ACKNOWLEDGEMENTS

I would like to thank my faculty advisor, Dr.Toliyat, for giving me this opportunity to study and work in the Advanced Electric Machines and Power Electronics Lab.

I would also like to extend my gratitude to my supervising graduate student and researcher, Matthew Gardner and Matthew Johnson, for their guidance and support throughout the course of this research.

Finally, thanks to my friends that have helped me with learning all the functions in SolidWorks and navigating the EDC.

# LIST OF TABLES

# LIST OF FIGURES

# CHAPTER I

# INTRODUCTION

Wind turbines convert kinetic energy of wind into electrical energy. Their use has greatly increased throughout the last decade. With this development, the reliability and functionality of the drivetrain must be addressed. In this research, the costs and benefits of using a magnetic continuously variable transmission as a drivetrain for wind turbines are studied.

## Drivetrain Systems

A primary component of the wind turbine is the drivetrain, the system that connects the wind turbine blades' power to the power grid. A challenge with drivetrains for wind turbines is that the frequency of the wind turbines' generated power must always match the power grid. There are three configurations to converting the frequency of the blades' rotor to the power grid frequency: direct-drive, gear-box, and a continuously variable transmission (CVT).

In a direct-drive system, the rotor blades directly drive the shaft of the synchronous generator. Large power electronics converters must convert all of the generated power to the grid's frequency and voltage. A more mechanically complex drivetrain system is the multi-stage mechanical gear-box. This is the most traditionally used drivetrain system for wind turbines. The gear-box adapts the low-speed rotor spun by the blades to the generator's speed. For this system, power electronics only need to be rated for the amount of power that is generated from the rotor currents, and the stator currents are fed directly to the grid. Though the size of the power electronics is decreased, gear-boxes require several mechanical gears to attempt to maximize the energy harnessed at a given windspeed.

A gear-less alternative for a drivetrain system is a continuously variable transmission (CVT). A CVT typically operates with a pulley system which allows for infinite variability between low and high gears. This is an especially desirable feature for wind turbines because windspeeds are also infinitely variable over a wide range [1]. CVTs have been increasing in implementation in vehicles; however, current studies are still working to design a CVT able to run for the long periods of time and handle high torques that wind turbines demand.

**Mechanical Gears**

The primary issue with the typical drivetrain is the use of mechanical gears. The interlocking teeth are required to transfer power between the shafts; however, the physical contact leads to several issues, such as noise, overload, heat, and wear-and-tear. For instance, micropitting, the development of microscopic cracks in gears, frequently happens to gears even at low speeds; however, they can be very difficult to detect as they are so small. With time and constant pressure, these cracks grow until the gear breaks. With mechanical gears, misalignment is always an issue; however, the impact of misalignment with wind turbines is severe. Wind turbines must keep the high-speed shaft at a speed such that its frequency matches the power grid. With mechanical gears, misalignment is always a potential issue; however, the impact of misalignment on wind turbines is severe [2]. Wind turbines must keep the high-speed shaft at a speed such that it synchronizes the AC power output from the turbine's generator with the power grid, and misaligned gears generally increases the rate of gear and bearing failure.

**Magnetic Continuously Variable Transmission**

Prior research corroborates that there are several potential advantages to using a magnetic continuously variable transmission (mCVT) as the drivetrain system instead of mechanical gears [3]. After a review of different configurations of the magnetic gears and how the parameters

may be optimized [4, 5] for efficiency, an axial magnetic gear configuration, shown in Figure 1, was chosen for this project. Existing analysis on traditional mechanical gears is used as a guide in understanding what parameters and situations are important in developing a reliable magnetic gear [6] for use in a wind turbine. Additionally, prior research on the benefits of using mCVTs for wind turbines has showcased several essential variables [7].

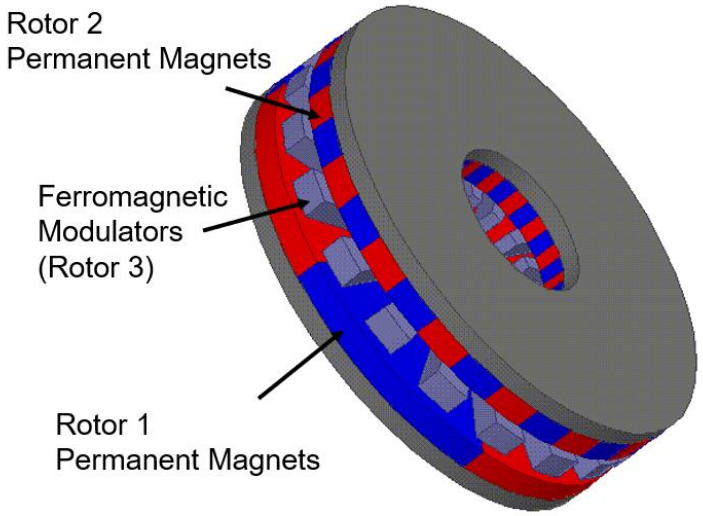


Figure 1. Axial Flux Permanent Magnet Gear.

With the use of an mCVT drivetrain, the three rotors of the magnetic gear correspond with the turbine blades, control rotor, and the synchronous generator rotor. In Figure 2, the synchronous rotor is connected to Rotor 1, the High-Speed Rotor (HSR). The wind turbine blades are connected to the modulators, Rotor 3. The control rotor is connected to Rotor 2, the Low Speed Rotor (LSR). Ultimately, all the parts of the mCVT work to harness power from the wind turbine blades and then convert it to match the frequency of the grid so that the power may be used.

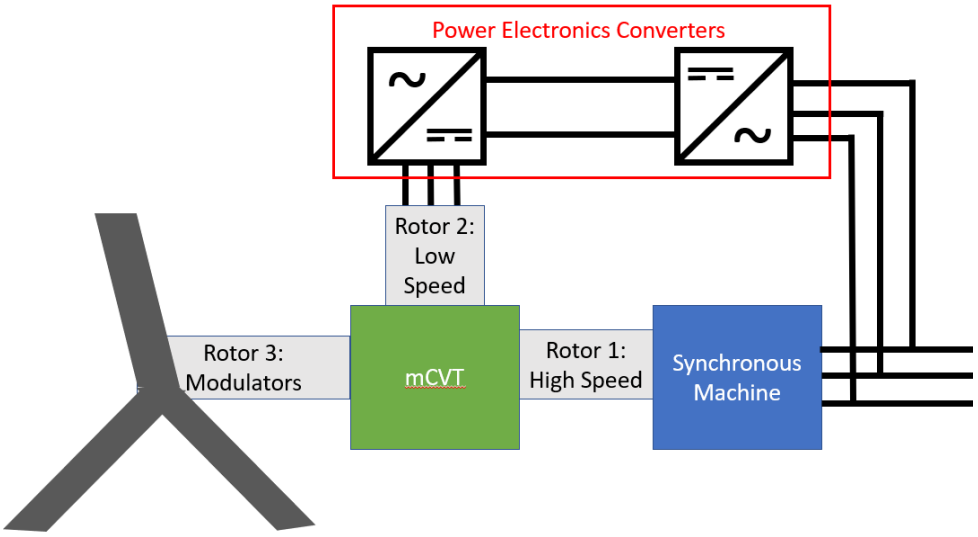


Figure 2. Magnetic Continuously Variable Transmission Drivetrain (mCVT).

In Figure 2, there are two primary modes of operation that depend on the wind speed. At low wind speeds, Rotor 3 does not supply enough speed to rotate Rotor 1 to match the grid frequency. Therefore, power must come from the grid, through the power electronics converters and Rotor 2. With both Rotor 2 and Rotor 3 rotating in the mCVT, Rotor 1 is guaranteed to rotate at a frequency matching the grid. The other mode of operation is when there are high wind speeds. At a certain wind speed, Rotor 3's speed will push Rotor 1 to a frequency above what the grid is rated. As a result, some of the power from Rotor 3 must be taken through Rotor 2, the power electronics, and to the grid to be used.

**Challenges with Magnetic Gears**

The implementation of mCVTs in wind turbines is impeded by the requirement of large and costly power electronics converters. Ideally, wind turbines would harness power at all windspeeds. In reality, for the mCVT to handle high and low wind speeds, a bidirectional converter required to allow the delivery of power to and from the power grid, thus increasing the size of the required power electronics. An additional issue of heavily relying on the power

electronics converters is that each stage results in a little power loss due to inefficiency in the parts. An option is to set the gear ratio and the synchronous speed such that the low windspeeds do not require the power to go from the grid to the control rotor. This single direction power flow would only require a unidirectional power electronics converter, reducing the size and cost of the drivetrain.

**Purpose**

A goal of this research is to create an axial flux magnetic gear prototype to demonstrate how the magnetic gear may be a solution to the issues faced with mechanical gears. Simulations are conducted to design a magnetic gear prototype that can demonstrate how the magnetic gears function without physical contact. In addition, a two-axis testbed is specially designed and fabricated to test the impact of misalignment and air gap variance on the magnetic gear prototype's operation. The importance of the prototype lies in the analysis of the impact of misalignment on the prototype's torque angle curve.

The primary purpose of this research is to study drivetrain reduction for wind turbines with mCVTs. Simulations are conducted to find optimal gear ratios and synchronous generator speeds with the determined low wind speeds. Over a spread of optimal gear ratios and synchronous generator speeds, the generated power is tracked to determine the impact of operating at different wind speeds. Power electronics are necessary for the function of mCVTs in wind turbine drivetrains, but with the data found in this research, there is greater clarity in what the trade-offs are to reduce the cost and size of the drivetrain.

# CHAPTER II

# PRINCIPLES OF OPERATION

The operating principle of the axial flux magnetic gear shown in Figure 1, includes three major parts. The high speed rotor (HSR) is the rotor with fewer pole pairs and a backiron. The low speed rotor (LSR) is the rotor with a greater number of pole pairs and a backiron. The modulators are the middle rotor in the magnetic gear. They are typically made up of a ferromagnetic material, and the number of modulator pieces, $M$, is the sum of the number of pole pairs in the LSR, $Q_{LS}$ and the number of pole pairs in the HSR, $Q_{HS}$, as shown in (1).

$$M = Q_{HS} + Q_{LS} \qquad (1)$$

There are several modes of operation for the axial configuration of magnetic gears created by fixing any or none of the three rotors. The prototype designed in this research operates with fixed modulators because it is the simplest to design and analyze. For the application of the magnetic gear in an mCVT, all three rotors are rotating.

There are several basic concepts about mechanical gears that are translatable to magnetic gears. A significant property of gears is their gear ratio. In Figure 3, the mechanical gear has seven teeth on one rotor and eleven teeth on the other resulting in a gear ratio of 7:11. Analogous to the teeth in mechanical gears are magnetic pole pairs and modulator pieces. Pole pairs are couples of adjacent positive and negative magnets on a rotor. Figure 4 shows a magnetic gear with 3 pole pairs on the HSR, 7 pole pairs on the LSR, and 10 grey modulator pieces. The red and blue magnet colors indicate the alternating adjacent north and south poles. In magnetic gears,

the gear ratio depends on the mode of operation. If the modulators are locked like in the prototype used in this study, the gear ratio, $G_p$, is the ratio between the pole pairs as seen in (2). If none of the rotors are locked like in the mCVT application, the gear ratio, $G_{WT}$, is not fixed between any two rotors.

Figure 3. Mechanical Gear with Interlocking Teeth and 7:11 Gear Ratio.

Figure 4. HSR with 3 pole pairs. 10 Modulator pieces. LSR with 7 pole pairs. (Left to Right)

$$G_p = -\frac{Q_{LS}}{Q_{HS}} \qquad (2)$$

There are several constraints when considering the values of $Q_{LS}$ and $Q_{HS}$. One is the torque ripple, the undesired periodic increase and decrease of torque during the operation of electric machines. In order to minimize torque ripple, a non-integer gear ratio is necessary.

Additionally, an even number of modulators is desired because the symmetry cancels out most of the net forces on the bearings.

For the wind turbine simulations, the synchronous generator is the high speed rotor, Rotor 1, the wind turbine blades are attached to the modulators, Rotor 3, and the low speed rotor, Rotor 2, serves as the control rotor and is driven by power electronics. Because Rotor 2 is controlled by the wind speed, its rotational speed, $\omega_3$, is predetermined as the range of average wind speeds for wind turbine operation which does not exceed 15 rpm [6]. Rotor 1 represents the synchronous generator and its speed, $\omega_1$, depends on the synchronous generator's number of pole pairs, $p_{synch}$, and the required frequency output, *f*, as shown in (3). For this research, the synchronous generator required frequency output is 60 Hz and without additional gearing any $p_{synch}$ can be used to get the variety of $\omega_1$in Table 1.

$$\omega_1 = f * \frac{60}{p_{synch}} \qquad (3)$$

Table 1. Synchronous Generator Speed with Different Generator Pole Pair Counts.

| $p_{synch}$ | 1 | 5 | 10 | 25 | 30 | 45 | 120 |
|---|---|---|---|---|---|---|---|
| $\omega_1$ [rpm] | 3600 | 720 | 360 | 144 | 120 | 90 | 30 |

Note: Variable ranges for simulations are discussed later in the paper.

In order to reduce the drivetrain size and cost, it is important to analyze the torque, force required to rotate an object, rotational speed, and power required of the control rotor with different gear ratios and synchronous generator speeds over a range of wind speeds. (4) shows the relationship between the three rotors' rotational speeds at steady state.

$$\omega_1 - G_{WT} * \omega_3 + (G_{WT} - 1) * \omega_2 = 0 \qquad (4)$$

From (5), the equation to determine the control rotor speed can be derived (5). The control rotor speed is significant to analyze because if it must rotate in the negative and the positive direction, a bidirectional converter is required in the power electronics increasing the drivetrain size and cost. The torque relationships in (5) – (8) are used in the analysis. For wind turbines, low and high torques have to be achieved at different wind speeds, so it is important to also include the torque of each rotor in this review.

$$\omega_2 = \left(\omega_3 - \frac{\omega_1}{G_{WT}}\right) * \frac{G_{WT}}{G_{WT}-1} \qquad (5)$$

$$\tau_1 = -\frac{T_3}{G_{WT}} \qquad (6)$$

$$\tau_2 = -\frac{G_{WT}-1}{G_{WT}}\tau_3 \qquad (7)$$

$$\tau_3 = \frac{P_3}{\omega_3} \qquad (8)$$

The power relationship for each Rotor *n* (*n* = 1, 2, 3) in (9) is also used in the simulations to determine the power of each rotor. The power of the control rotor, $P_2$, is a focus of the analysis because the higher the maximum power, the higher the power electronics converters need to be rated which leads to a more expensive drivetrain.

$$P_n = \omega_n * \tau_n \quad (10)$$

# CHAPTER III

# PROTOTYPE METHODS

## Prototype Design

A major objective of this study is to look at the effects of misalignment on magnetic gear operation. The impact of misalignment on mechanical gears can be detrimental to their use in wind turbines. To be a viable solution to the issues faced by mechanical gears in wind turbines, the impact of misalignment on magnetic gears must be tested to prove that they are less severely impacted by misalignment. Another interesting measurement is the impact on air gap variance on the magnetic gear operation. A prototype and testbed were developed to test and validate the impact of these variances.

Simulations were done with ANSYS Maxwell to design a magnetic gear prototype that would demonstrate the impact of misalignment and air gap variance and had realistic specifications for fabrication and assembly. There is a tradeoff between physical magnet size and the ability to easily gather data. With larger magnets, greater steps of misalignment can be made and the torque and force can still be measured; however, assembly becomes significantly more difficult the larger and stronger the magnets are.

With ANSYS Maxwell, simulations of magnetic gears were done for several different magnetic gear designs, and the data acquired was filtered to determine which specifications were optimum for assembly and testing. Table 2 defines the most important variables used in the simulations. Figures 5-10 show the impact of the variables on the torque and axial force of the HSR and the LSR.

Table 2. Significant Simulation Variable Definitions.

| **Variable** | **Definition** |
|---|---|
| T1 | HSR Backiron Thickness |
| T2 | HSR Magnet Thickness |
| T3 | HSR Air Gap Thickness |
| T4 | Modulator Thickness |
| T5 | LSR Air Gap Thickness |
| T6 | LSR Magnet Thickness |
| T7 | LSR Backiron Thickness |
| P1 | HSR Pole Pairs |
| P2 | LSR Pole Pairs |

Note: Variable names and definitions are interchangeably used in the following plots.

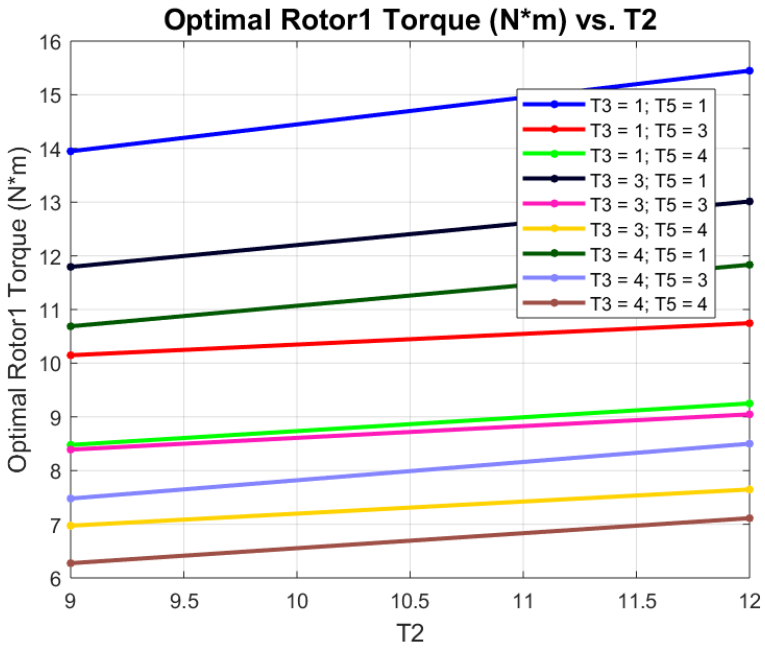


Figure 5. HSR Torque vs HSR Magnet Thickness in Families of Air Gap Thicknesses.

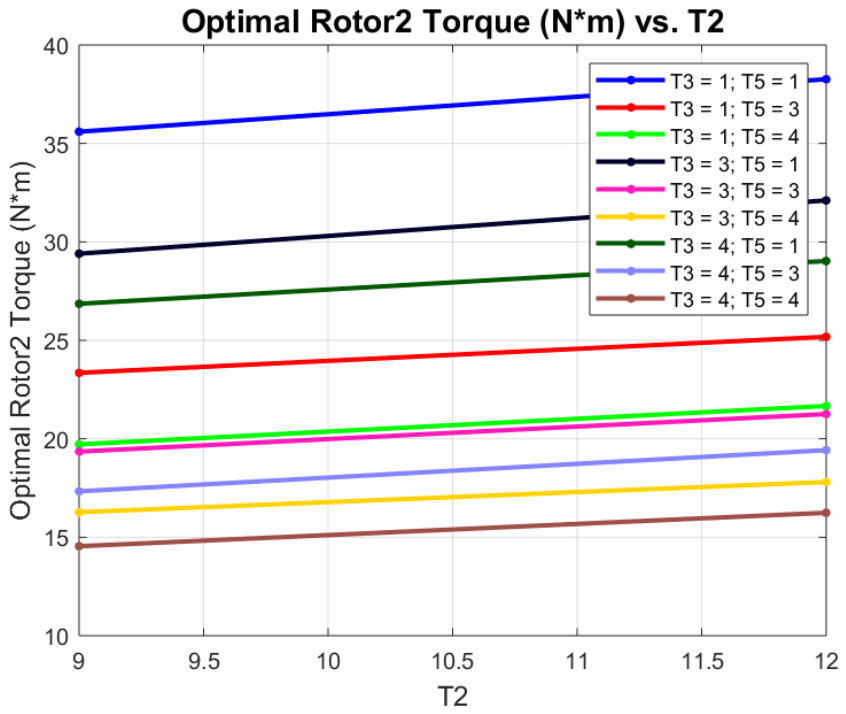


Figure 6. LSR Torque vs HSR Magnet Thickness in Families of Air Gap Thicknesses.

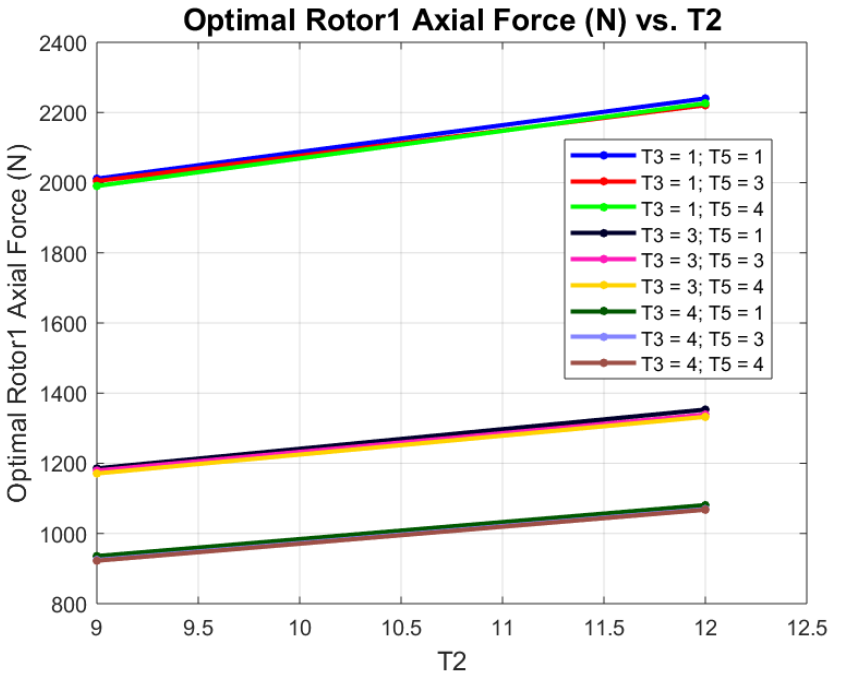


Figure 7. HSR Axial Force vs HSR Magnet Thickness in Families of Air Gap Thicknesses.

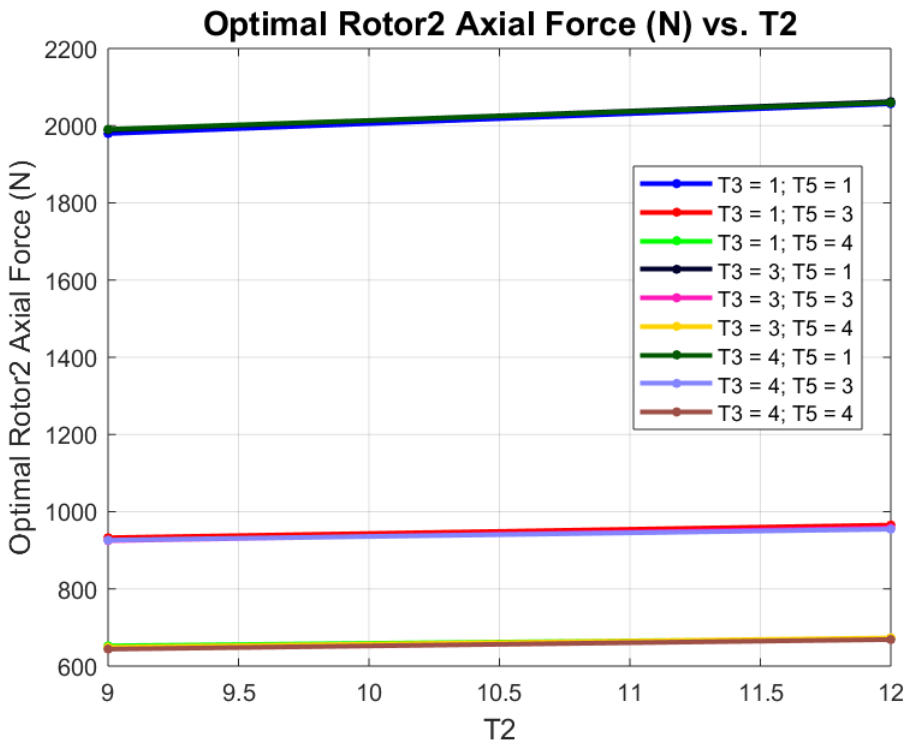


Figure 8. LSR Axial Force vs HSR Magnet Thickness in Families of Air Gap Thicknesses.

Figures 5-8 have lines that are color coded according to the air gap between the LSR and Modulators and between the HSR and Modulators. From the figures, it can be seen that as the air gaps are increased, the torques and axial forces decrease, and as the HSR and LSR magnet thicknesses increase, the torques and axial forces increase. The simulations were done up to an air gap of 4mm, but the prototype is tested up to 10mm. The plots were used to make sure that for the selected magnet thickness, a large air gap will still result in a measurable torque and axial force during testing.

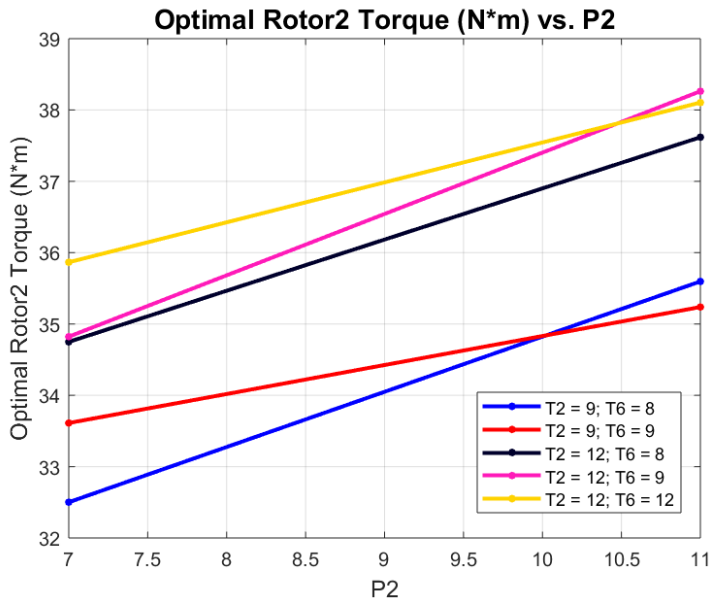


Figure 9. LSR Torque vs LSR Pole Pairs in Families of Magnet Thicknesses.

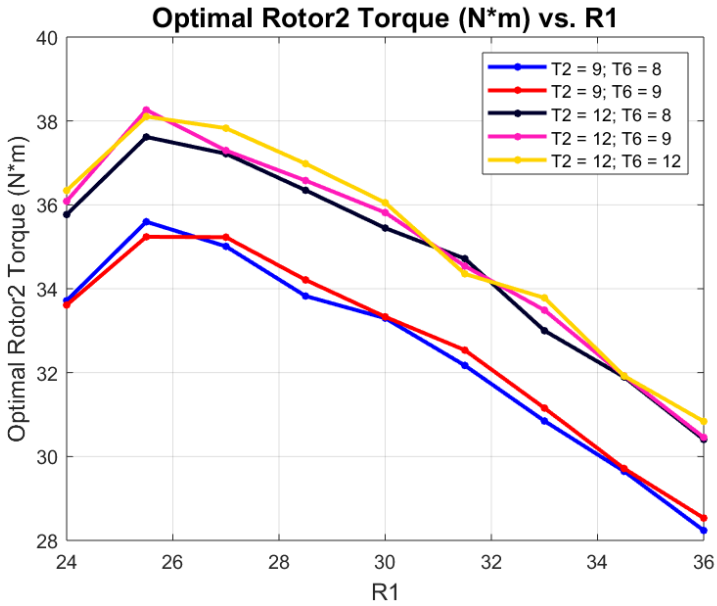


Figure 10. LSR Torque vs Inner Radius in Families of Magnet Thicknesses.

Figure 9 shows the impact of varying the LSR pole pairs. For the simulations in that figure, HSR pole pairs were held at 3 and air gaps were held at 1mm. The plots indicate that at a

certain number of pole pairs, it is better to have less thick magnets. While the maximum outer radius is 60mm due to the lab's available materials, the inner radius was varied in the simulations to view the optimum value to get the greatest torque. The impact of the inner radius size on the torque is shown in Figure 10.

In order to physically assemble the magnetic gear, several limitations were set at the start of the prototype design. As mentioned in the Principles of Operation, a non-integer gear ratio was chosen, $Q_{HS}$ and $Q_{LS}$ were limited to a maximum of 10 in order to prevent having to handle over 20 magnet pieces per rotor, the magnet thickness could not exceed 12mm to minimize the dangers of setting the magnets, and the outer radius of the entire gear was limited to 60mm due to the lab's available material. These constraining factors are listed in Table 3.

Table 3. Prototype Design Constraints.

| **Parameters** | **Constraint** |
|---|---|
| Magnet Thickness | <= 12 mm |
| Backiron thickness | < 20 mm |
| Outer Radius | < 60 mm |
| HSR Pole Pairs | <= 10 |
| LSR Pole Pairs | <= 10 |
| Modulator Pieces | <= 20 |
| LSR Torque | 20-40 Nm |
| HSR Torque | 5-10 Nm |

After several simulations of different magnetic gear prototype designs, the chosen specifications were decided and are listed in Table 4. The selected parameters are within the physical constraints in Table 3 and the simulations indicate that they will give measurable torques and axial forces with different misalignments and air gaps for testing.

Table 4. Chosen Magnetic Gear Prototype Design Specifications.

| **Parameters** | **Constraint** |
|---|---|
| Magnet Thickness | 12 mm |
| Backiron Thickness | 20 mm |
| Modulator Thickness | 9 mm |
| Inner Radius | 24 mm |
| Outer Radius | 60 mm |
| HSR Pole Pairs | 3 |
| LSR Pole Pairs | 7 |
| Modulator Pieces | 10 |

Note: Number of HSR and LSR magnet pieces are two times the HSR and LSR Pole Pairs.

Using the parameters in Table 4, the magnetic gear prototype was fabricated and assembled. For fabrication, tolerance had to be included in the magnet pieces which resulted in small gaps between the magnets. With the LSR, shims had to be used as shown in Figure 11 to prevent the build up of a large gap between two magnets which would impact the operation of the magnet. The HSR did not require shims because there are fewer pieces resulting in a smaller number of areas for error.

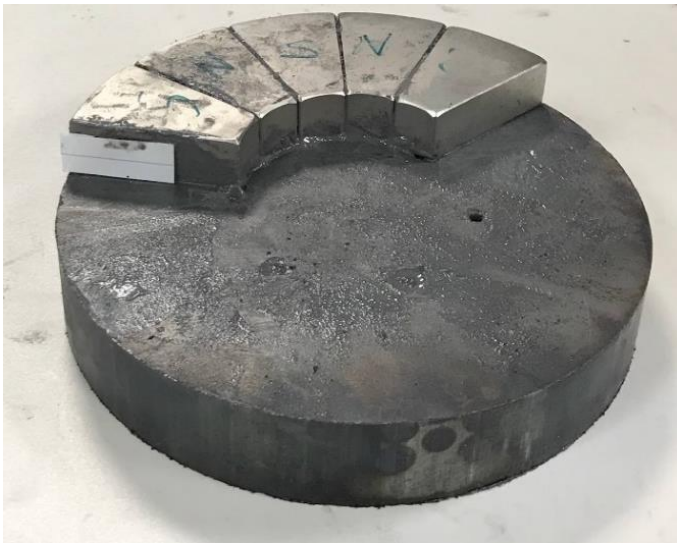

Figure 11. White Shims Between Magnets on the LSR.

The magnets naturally stick to the backiron; however, an epoxy was also used to ensure the magnets were adhered to the backiron. As a precaution against the magnets flying off the backiron during fast rotational speeds, a Delrin sleeve was designed to encase each rotor as shown in Figures 12 and 13.

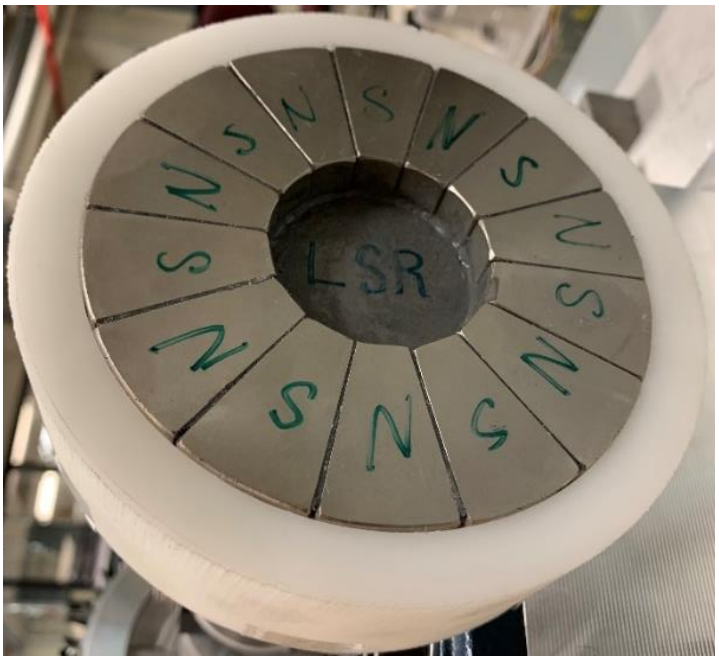


Figure 12. LSR with Labeled North and South Poles.


Figure 13. HSR with Labeled North and South Poles.

**Modulator Case Design**

Due to the size of the prototype and the purpose to manipulate the airgap size, there is little space between the rotors to have supporting structures to hold the modulator and magnet pieces in place. Garolite, a fiberglass epoxy laminate, was the material chosen for the modulator case. The Garolite was used in the ANSYS Workbench simulation to determine whether it could hold the modulators in place against the pull of the magnetic gear. Figure 14 shows the stress on the modulator case, and Figure 15 shows the deformation of the case with the modulators inside the case and the magnets pulling on either side.

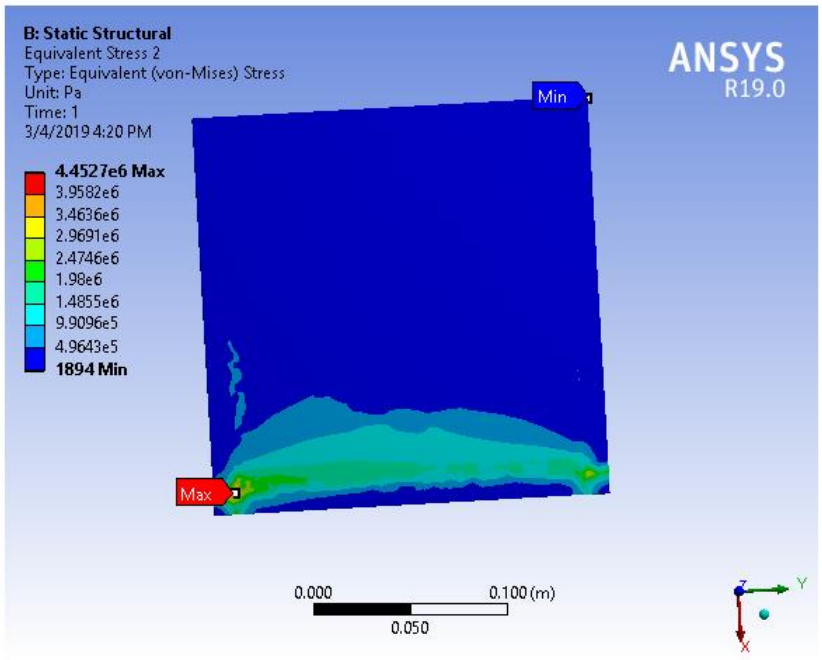


Figure 14. Static Structural Stress Test on Garolite Modulator Case.

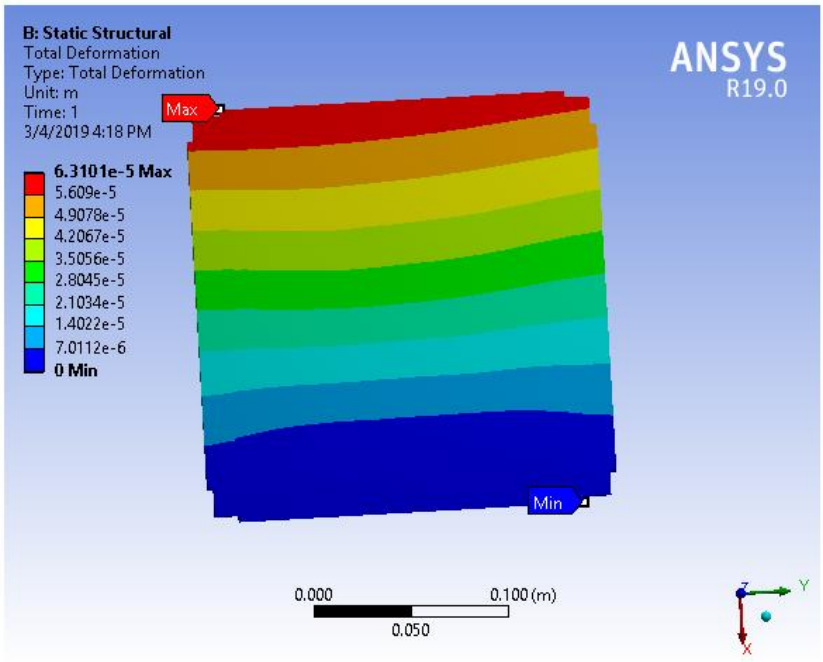


Figure 15. Static Deformation Test on Garolite Modulator Case.

Ideally, to have the least amount of deformation, the Garolite would be as thick as possible, but a requirement of the prototype is to achieve a measurable torque. With the ANSYS Workbench simulations, the thickness of the Garolite was varied to find the optimum thickness to hold the modulators in place. Additionally, the length and height of the modulator case, was manipulated in order to determine if the angle irons used to seal the edges of the modulator case were within the magnetic field, influencing the operation of the magnets. The chosen specifications for the modulator case are listed in Table 5 and result in less than 1 mm of deformation. The deformation was of great importance to minimize because for this research, a priority is to maintain a constant and known air gap to determine the impact of air gap variance on the magnetic gear operation.

Table 5. Modulator Case Specifications.

| **Parameter** | **Value** |
|---|---|
| Length | 203.2 mm |
| Height | 203.2 mm |
| Thickness | 12.7 mm |

Note: Values are rounded from inches to millimeter conversion.

Figure 16 shows the designed modulator case in green and its stand created in SolidWorks. The figure has the front half of the Garolite set to transparent for the purpose of showing the modulators configured inside. The stand is designed to be bolted to a T-slot table. With this design, the modulators can be fixed between the magnetic rotors.

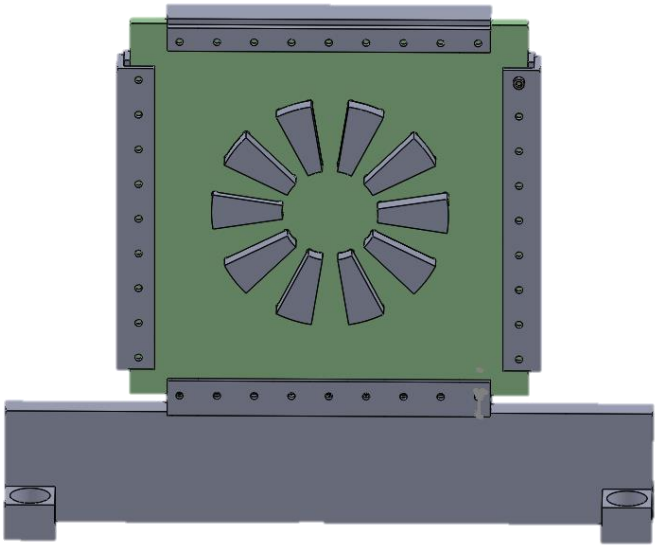

Figure 16. SolidWorks Model of Modulator Case and Base.

After the modulator case was tested and finalized in ANSYS and SolidWorks, it was fabricated and assembled. Figure 17 shows the Garolite case with the Modulators placed, and Figure 18 shows the Garolite closed without the angle irons clamping them closed.

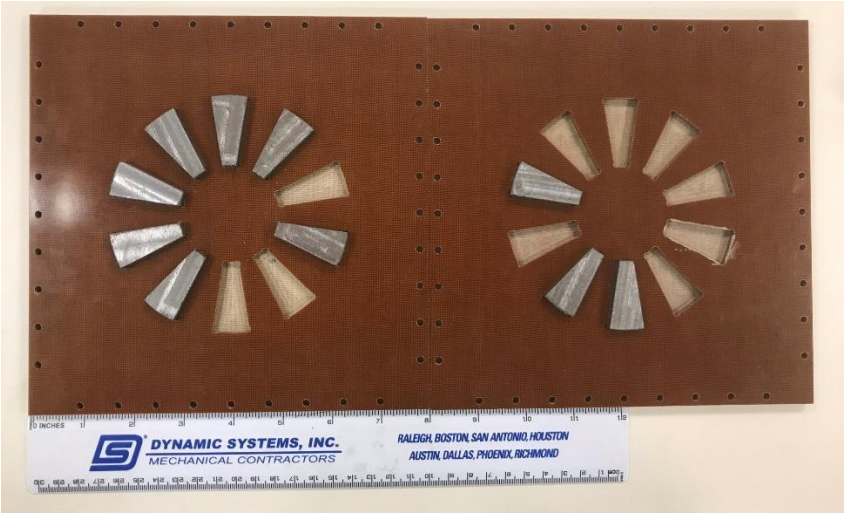


Figure 17. Open Garolite Case with Modulator Pieces Laid.

Figure 18. Unclamped Modulator Case.

After the modulators were clamped, they were screwed onto the modulator base as shown in Figure 19. Although the Garolite behaved like the simulations indicated, the side angle irons were replaced with larger steel slats to more securely hold the modulator case upright when the magnets were brought close as shown in Figure 20.

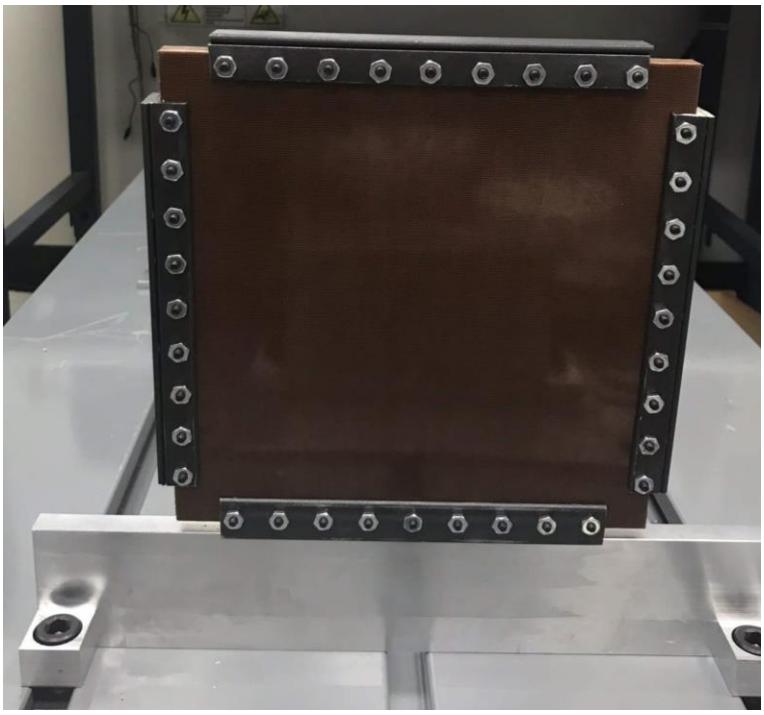

Figure 19. Mounted Modulator Case and Base.

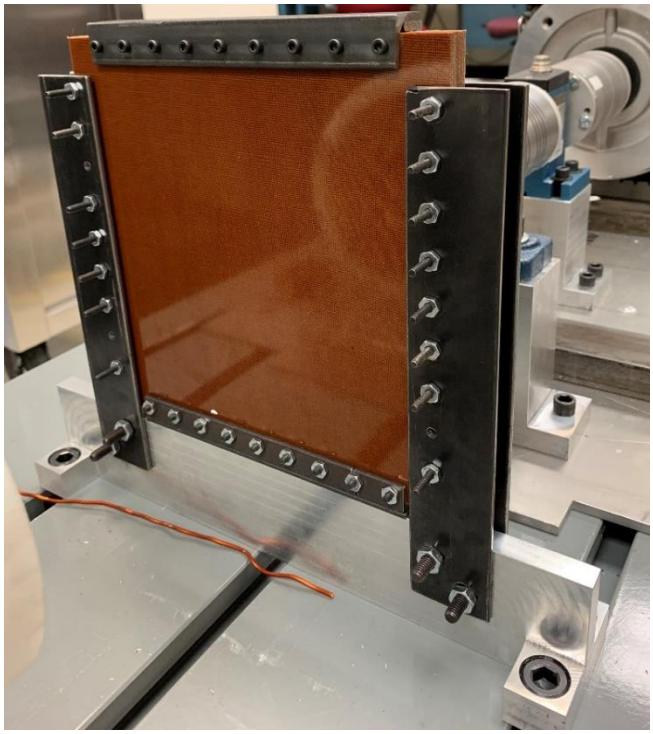

Figure 20. Mounted Modulator Case and Base with Reinforced Side bars.

**Testbed Design**

The testbed is designed of three primary parts, the base to hold the modulators stationary, and two sliding plates each designed to move along two axes and carry a 200 lb. motor, torque meter, and a magnetic rotor. Figure 21 shows the conceptual design on the testbed with labeled dimensions.

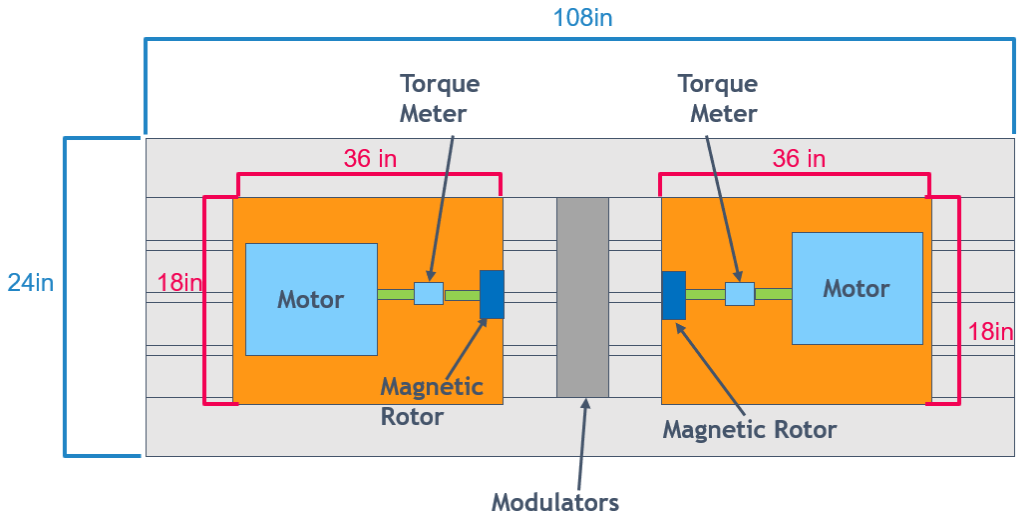


Figure 21. Conceptual Testbed Design with Dimensions.

In order to meet the precision requirement to adjust the testbed 10mm in each direction, the testbed was designed with M10x1mm screws. One full rotation of the screw results in one full millimeter of axial movement. For example, to move the testbed in Figure 22 to the left 2mm, screws 1-3 would be unscrewed two full turns then screws 4-6 would be tightened two full turns. To change the air gap, screw 7 can be tightened to pull the sliding plate towards the back bar or loosened to allow the sliding plate to be pushed forward.

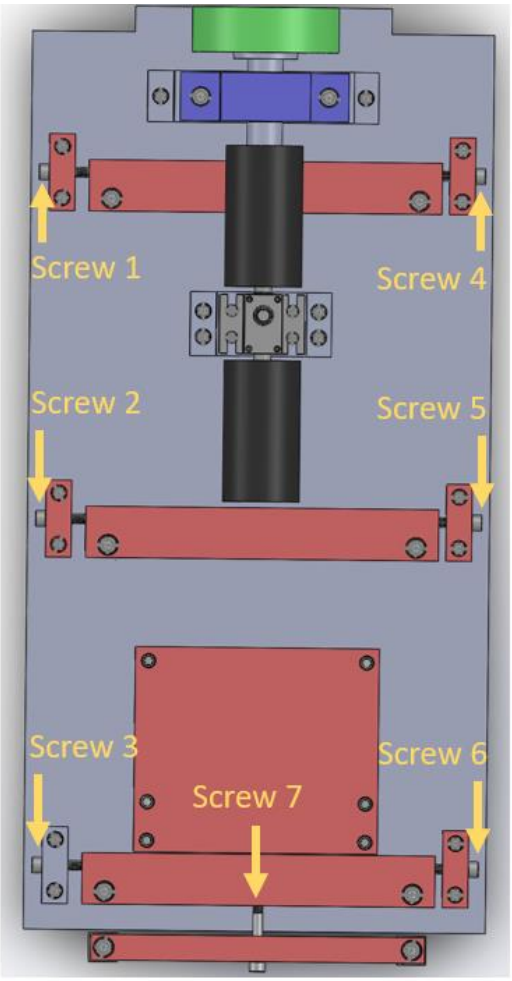


Figure 22. Testbed Arial View with Labeled Adjustment Screws.

The testbed shown in Figures 23 and 24 was designed in SolidWorks so that the sliding plates may hold the weight and size of the motor, torque meter, and magnetic rotor, and move independently from one another along two axes on the t-slot table. The cuts in the front of the sliding plate allow room for the sliding plate to move at least 10mm axially to adjust misalignment and to leave room for the modulator stand's feet.

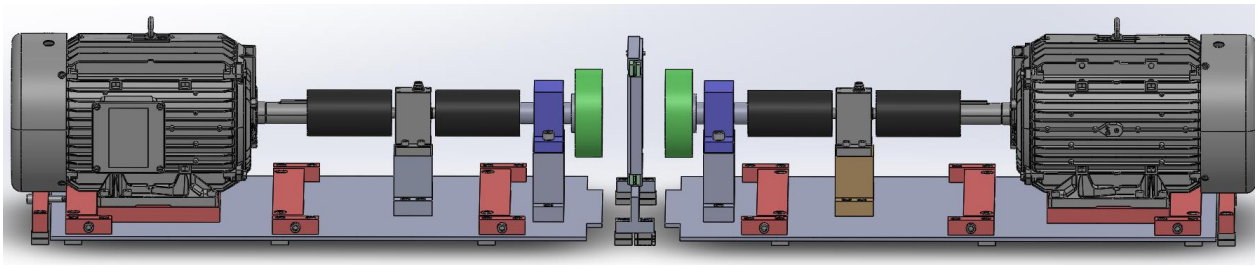

Figure 23. SolidWorks Model of Testbed and Prototype – Side View.

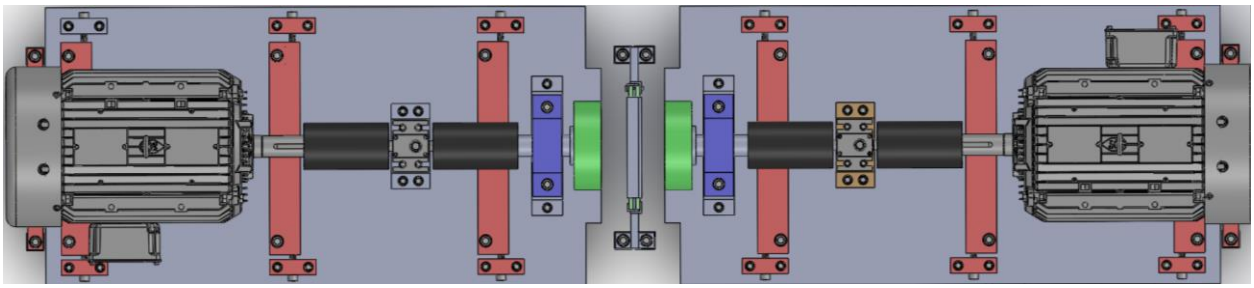

Figure 24. SolidWorks Model of Testbed and Prototype – Aerial View.

After ensuring all the parts on the SolidWorks model fit together, the parts were fabricated and assembled as shown in Figure 25. Figure 26 shows a closer view of the three rotors with a physical air gap between them.

Figure 25. Fully Assembled Testbed and Prototype.

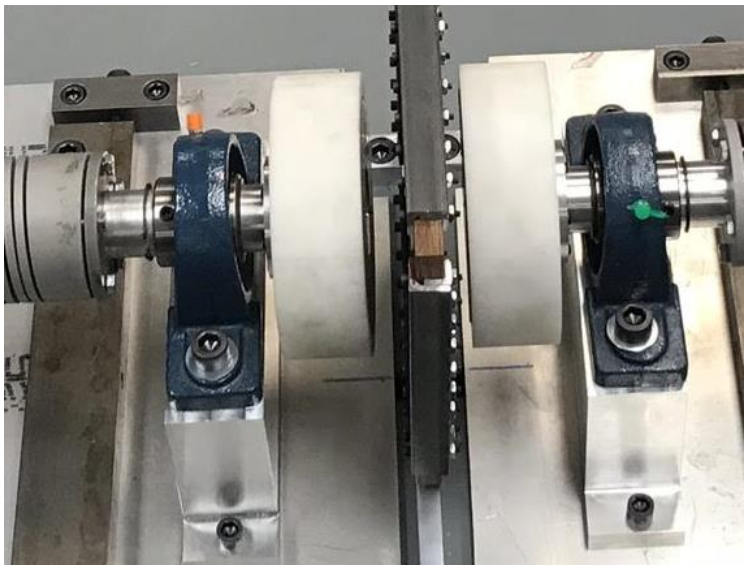

Figure 26. Close View of Three Rotors and Physical Air Gap.

The testbed moved along two axes as expected, and Figure 27 shows the testbed misaligned at 10mm on each side. Because of the weight of the motors and the use of the T-slot table, the testbed requires movement in small increments.

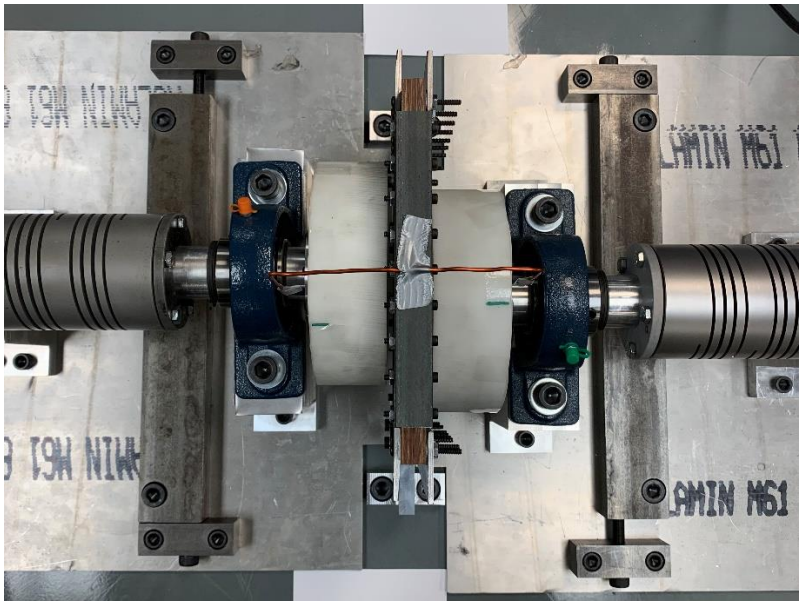

Figure 27. Sliding Plates Misaligned 10mm in Each Direction.

# CHAPTER IV

# PROTOTYPE RESULTS

With a mechanical gear, slipping gears results in teeth breaking and then requiring time and money to replace the broken gears. With magnetic gears, if the gears slip, the magnets merely recouple with the next pole pair. A torque angle curve shows the amount of torque required to turn the magnetic gear a certain number of degrees. It is sinusoidal shaped because at a maximum angle, the gear reaches its peak torque. For magnetic gears, this peak torque is the slip torque. As it slips passed the peak maximum angle, the torque decreases until it reaches the next maximum angle for the current magnet and slips again.

With the prototype and testbed assembled and calibrated, test cases were reviewed and executed. The air gap was locked at 5.6mm on the LSR side and 8.1mm on the HSR side. With the chosen magnetic gear parameters and set air gaps, simulations were done to get the expected torque vs. torque angle curves. The torque was measured at each angle to gather the experimental torque vs. torque angle curve. Figure 28 include the directions for positive and negative movement of the testbed relative to the modulators at the center.

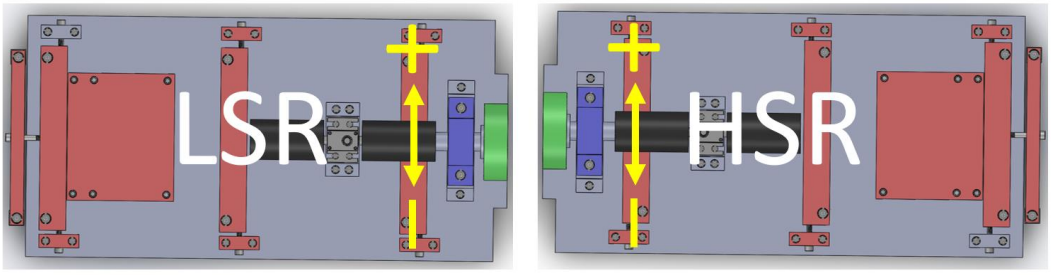


Figure 28. Testbed with Defined Misalignment Directions.

Because the sliding plates move -10mm to 10mm, the data for reflected scenarios are the same. For example, -10 mm on the LSR and -4 on the HSR gives the same results as 10mm on the LSR and 4 on the HSR. Therefore, the data shown in this paper will only include data with the LSR misalignment in the range -10mm to 0mm to avoid clutter. Figure 29 shows the simulated data for all cases, and Figure 30 shows the experimental data for all cases.

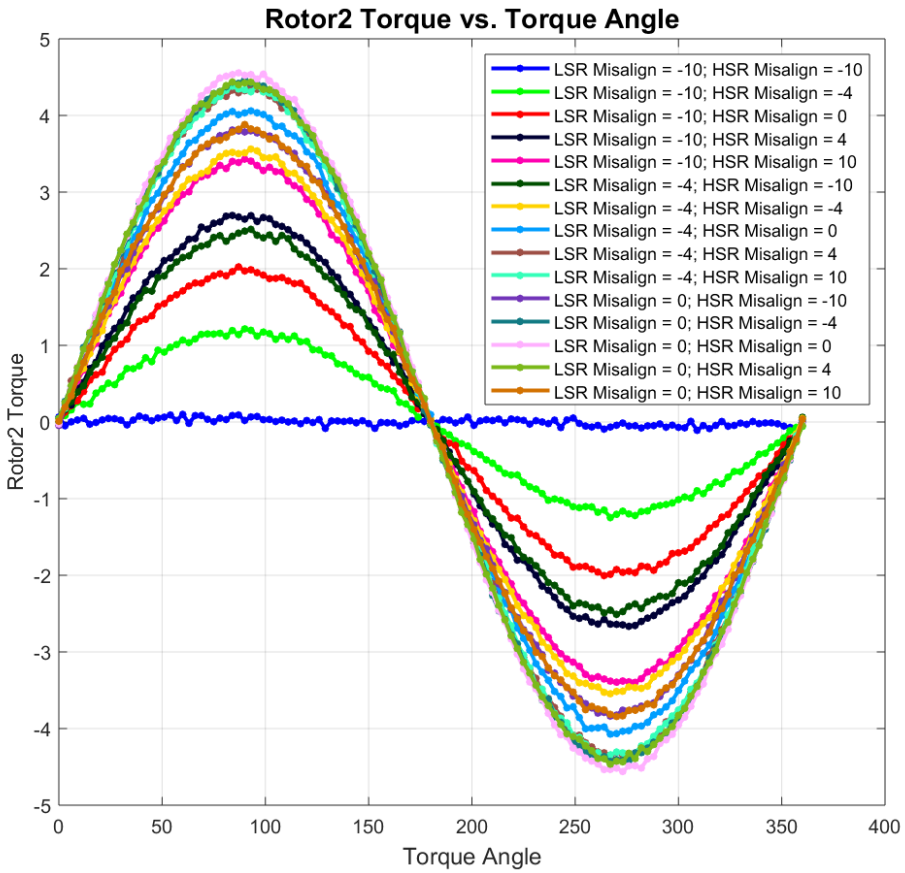


Figure 29. All Simulated Torque Angle Curve.

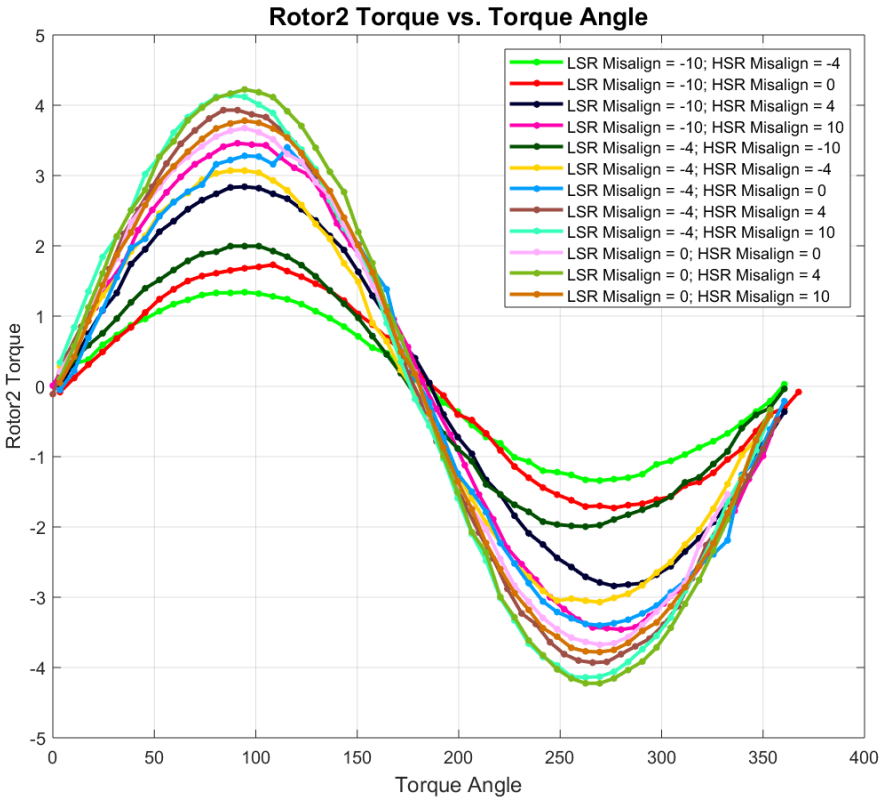


Figure 30. All Experimental Torque Angle Curve.

With the misalignment, it is anticipated that the operation of the magnetic gear will deteriorate, so a difference in peak torque and deformation of the sine curve is expected. Figure 31 shows the torque angle curves of the misalignment configurations that show a drop in peak torque angle. The Data type variable toggles from 0 to 1 with 0 indicating simulated data and 1 indicating experimental data.

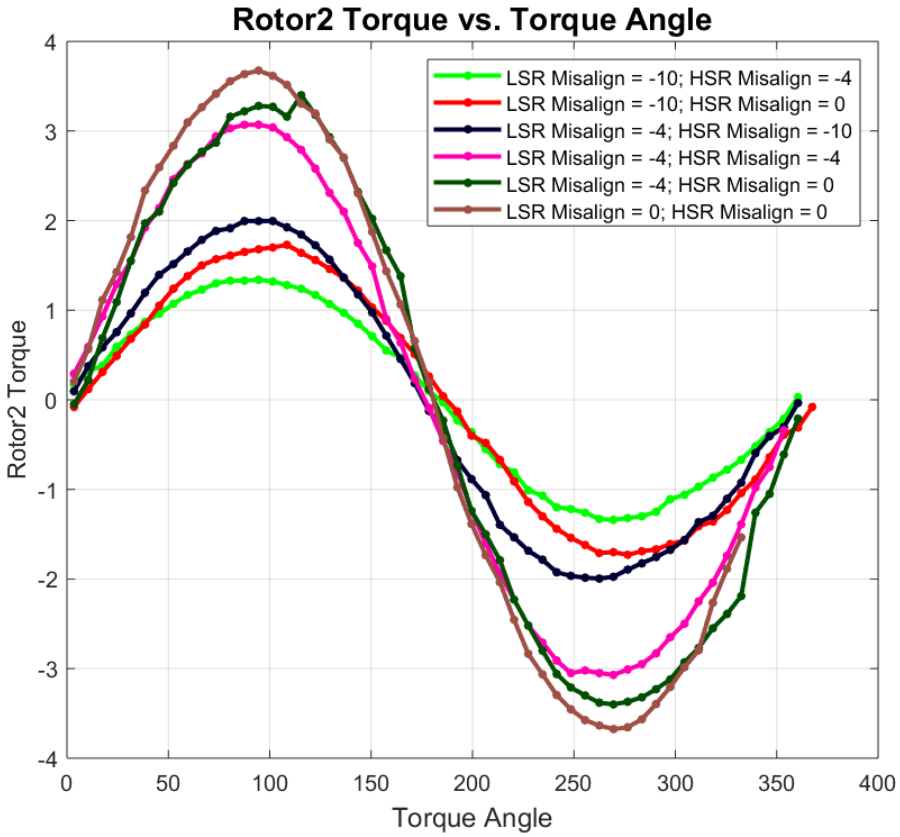


Figure 31. Peak Amplitude Loss with Misalignment.

The peak torque amplitudes for each misalignment configuration are listed in Table 6, and the deviation of the peak torque from the peak torque with no misalignment is shown in Figure 32. The deviation of the peak torque is worst for the cases where the misalignment is in the same direction. Interestingly, when the misalignment is in the opposite direction, the impact on the peak torque is not as severe.

Table 6. Peak Torque with Each Misalignment Case.

| LSR Misalign / HSR Misalign | 0mm | -4mm | -10mm |
|---|---|---|---|
| **-10mm** | | 1.995 Nm | |
| **-4mm** | | 3.07 Nm | 1.34 Nm |
| **0mm** | 3.675 Nm | 3.4 Nm | 1.73 Nm |
| **4mm** | 4.225 Nm | 3.93 Nm | 2.84 Nm |
| **10mm** | 3.78 Nm | 4.14 Nm | 3.46 Nm |

Note: Gray boxes are misalignment combinations that are symmetrical to values already tested.

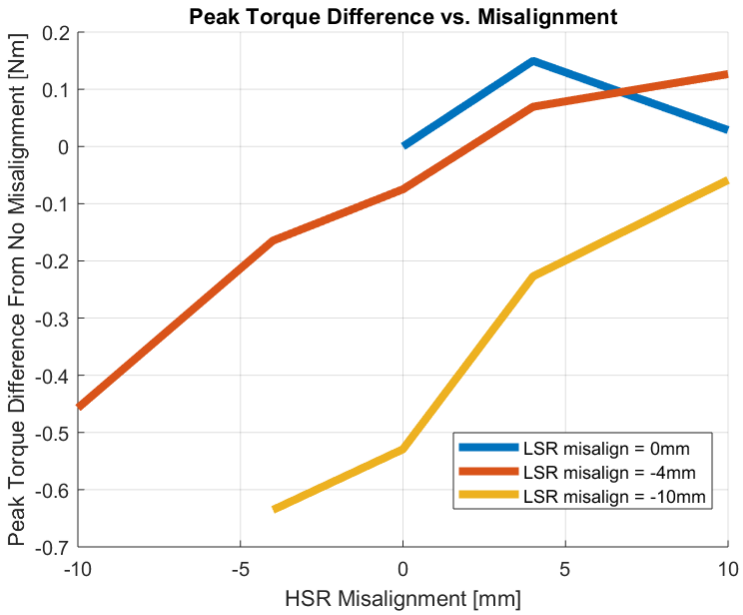


Figure 32. Peak Torque Deviance from No Misalignment.

The simulated data and experimental data are compared in Figures 33 and 34. There are some simulations with a greater percentage of error than others. This may be attributed

misalignment of the shaft relative to the sliding plate. The misalignment is determined based on the sliding plate relative to the T-slot table it is mounted on. Future designs of the testbed will have points of calibration closer to the magnetic rotor to the modulators for greater accuracy.

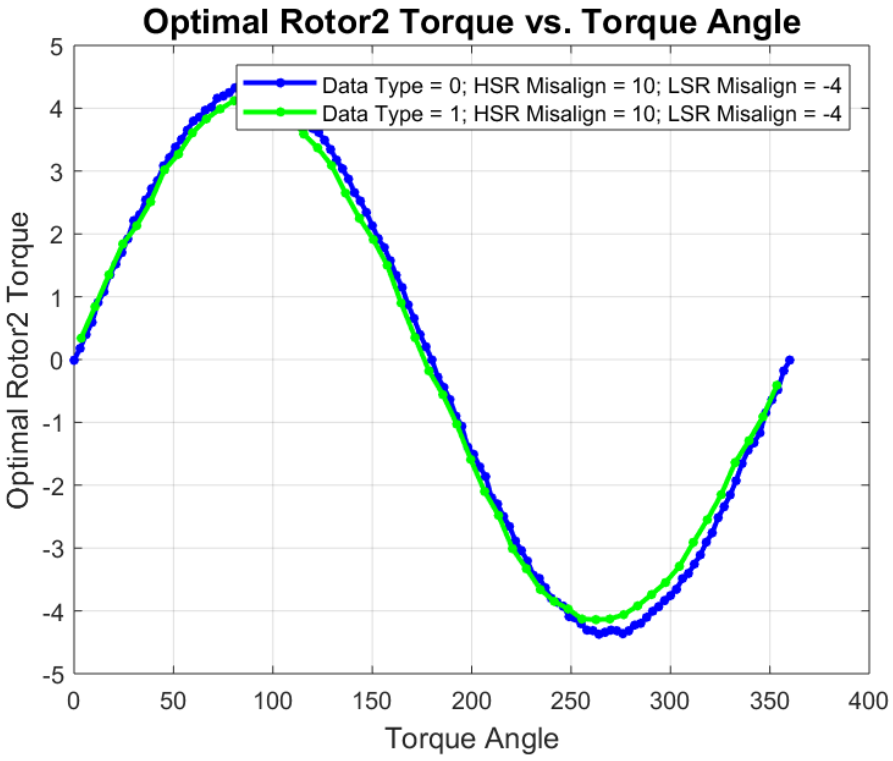


Figure 33. Simulated and Experimental Data with a Small Percentage of Error (4.4%).

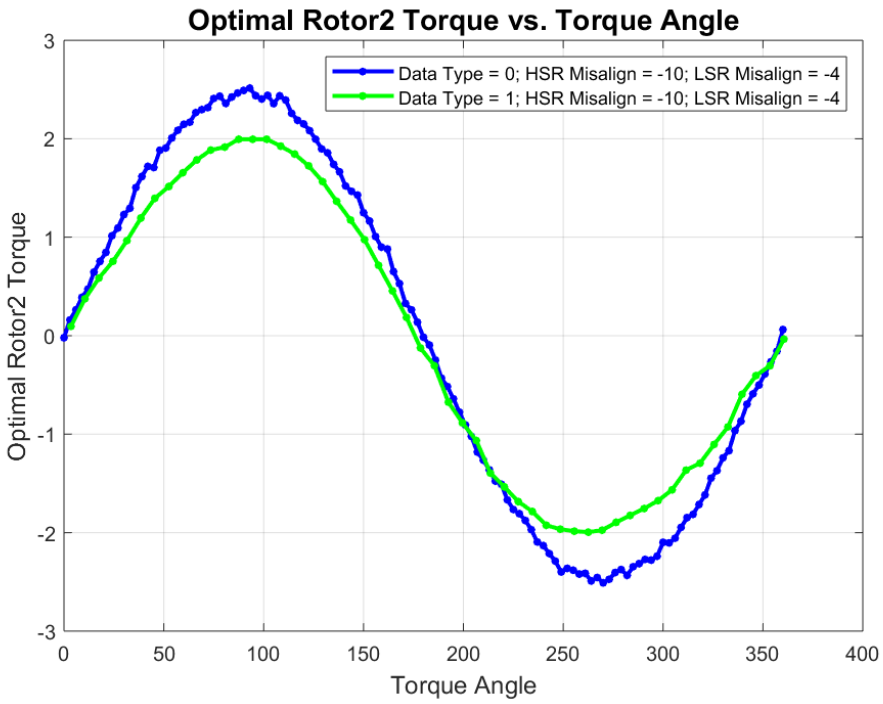


Figure 34. Simulated and Experimental data with a Larger Percentage of Error (9.8%).

Misalignment in gears causes a deviance from the expected torque angle curve. Typically, a drop in the slip torque is expected which is undesirable because the gear then functions at a lower torque rating than it is designed to. With the drop in peak torque, the gear is more prone to slipping. Although slipping magnetic gears is as not detrimental to the system as it is for mechanical gears, it is still not a desirable incident. The acquired experimental data shows that the impact of misalignment does alter the torque angle curve as expected; however, for some instances of misalignment, the slip torque increased. This does not agree with the simulation data, and is most probably attributed in imprecision in measuring the misalignment on the prototype.

# CHAPTER V

# WIND TURBINE ANALYSIS METHODS

In order to use a magnetic continuously variable transmission in wind turbines, power electronics converters are required. A major portion of this research is dedicated to the reduction of the cost and size of the power electronics converters. For this research, rotor 1 is the high speed rotor (HSR) connected to the synchronous generator, rotor 3 is connected to the wind turbine blades, and rotor 2 is the low speed rotor (LSR) connected to the control rotor. The synchronous generator must operate at a frequency matching the power grid it is connected to, and the wind turbine blades rotor's speed is dictated by the wind speed. The function of the control rotor is to use power electronics converters to supplement the power provided by the wind turbine blades to match the synchronous generator.

A bidirectional converter allows the control rotor to handle supplying power when the wind turbine blades are not harnessing enough power and feeding the excess power through the control rotor and power electronics to the power grid when there are high winds. Using a unidirectional power electronics converter instead of a bidirectional converter is one option to reduce the size of the drivetrain. With this solution, the control rotor is no longer able to handle both operating scenarios. Typically, the windspeed has to be very low to require the control rotor to supply power, additionally, if the power flows from the grid through the power electronics, through the control rotor, to the synchronous generator, some power is lost because of inefficiencies at each stage. Therefore, if only one direction of power flow through the control rotor is permitted, putting power into the grid the ideal direction. Thus, for this research as described in Figure 35, the power away from the mCVT is the positive power. Power supplied

from the grid to supplement the power harnessed at low wind speeds is an undesired scenario and is the negative power.

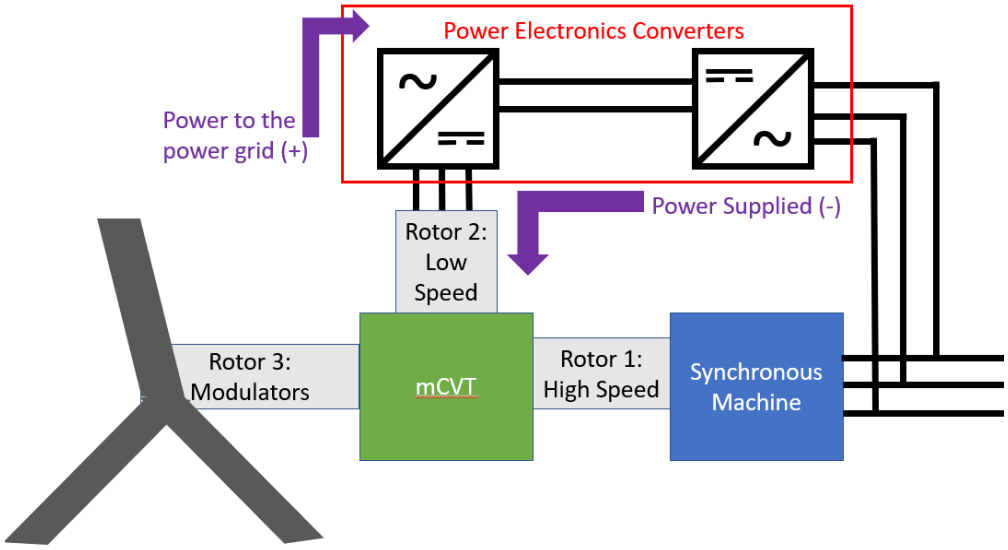


Figure 35. Power Flow with Power Direction Defined.

Another opportunity to decrease the power electronics converter cost is to minimize the power rating required of the control rotor. If the control rotor must handle a great volume of power, the power electronics must be rated for greater power. Larger power rating is proportional to the cost of power electronics, so in this study, the maximum power required of the control rotor is considered.

The cut-in speed is the windspeed at which the wind turbine begins harnessing power. Unless the windspeed reaches the cut-in speed, the wind turbine blades either simply rotate without harnessing power or they remain tethered. To simulate only using a unidirectional converter, the cut-in speed is adjusted to wherever the control rotor power is only positive. Figure 36 shows a Power Relationship vs. Windspeed curve with the cut-in speed marked for a

unidirectional power electronics converter. The notable trade-off with raising the cut-in speed is that areas primarily have windspeeds below that cut-in speed will spend the majority of the time with their wind turbines not producing power.

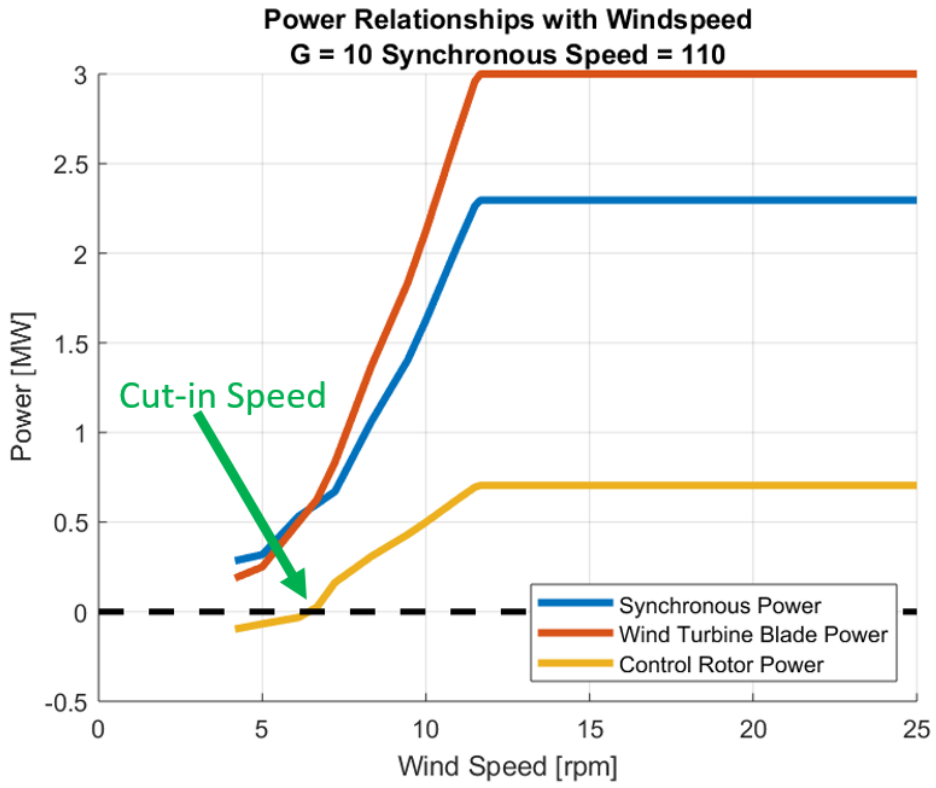


Figure 36. Power Relationships with Windspeed with Cut-in Speed Labeled.

For an mCVT in a wind turbine, a common challenge is trying to reach high torque at low rotational speeds and low torque at high rotational speeds. In most motors, back emf voltage controls the rotational speed and current controls the current. Field weakening is a method that is essentially a trade between current and voltage, essentially sacrificing torque for speed. Figure 37 shows an example of a scenario that requires field weakening. The torque at point A is smaller than at point B, but the magnitude of the rotational speed is substantially larger at point

A than the rotational speed at point B. This would require a great amount of field weakening to allow the motor to function at both the low and high wind speeds. Although field weakening is a method that allows for the tradeoff between voltage and current for the purpose of reaching high and low torques at high and low rotational speeds, all machines have a limit to how much they can field weaken [8].

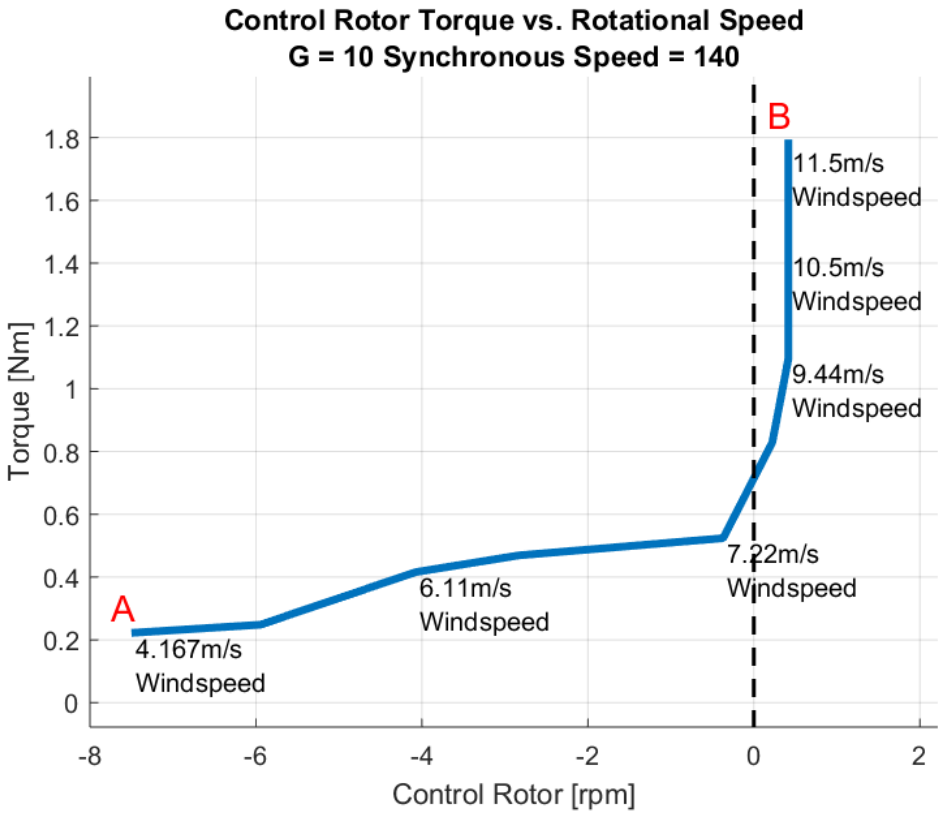


Figure 37. Torque vs Control Rotor Speed to Requiring Field Weakening.

In order to observe the power rating, cut-in speeds, and field weakening required of different scenarios, this study presents data primarily in the form of the Power Relationship plots and the Control Rotor Torque vs. Rotational Speed plots. Table 7 shows the ranges for controlled variables in the scenarios.

Table 7. Wind Turbine Variable Ranges.

| **Parameter** | **Range** |
|---|---|
| Windspeed [m/s] | 0-25 |
| Blade Speed [rpm] | 7-15 |
| Wind Power Generated [MW] | 0-3 |
| Gear Ratio | 2-14 |
| Synchronous Generator Frequency [Hz] | 60 |
| Synchronous Generator Pole Pairs | 15-90 |
| Calculated Synchronous Generator Rotational Speed [rpm] | 40-240 |

Note: Step sizes between variable ranges vary.

Typically, synchronous generator frequencies are set to 50 Hz or 60 Hz, but to simplify the simulations, only one frequency will be used. To simplify the calculation of plausible synchronous generator rotational speeds using (4), pole pairs are selected that are result in integer rotational speeds. Although the range of possible rotational speeds is wide, the focus will be on the simulations that demonstrate an impact on power rating, field weakening, and cut-in speed for a system with a unidirectional converter. Analyzing the impact of changing the synchronous generator speed and gear ratio on the behavior of the plots will allow for greater understanding of how to minimize the drivetrain size and cost in wind turbines.

# CHAPTER VI

# WIND TURBINE ANALYSIS RESULTS

In order to most efficiently move through the cases, all of the scenarios will initially have a gear ratio of 10 and adjust the synchronous generator speed from the minimum to maximum listed speeds in Table 7. The speed ratio between the minimum and maximum torques will be used as the indicator for field weakening. Most motors can field weaken within a 10:1 speed ratio [8]. The power ratio and cut-in speeds for each case will also be discussed.

**Case 1**

Figures 38 and 39 are the Power Relationship plot and the Torque vs. Rotational Speed plot, respectively. With a synchronous generator speed of 40 rpm, the control rotor only handles positive power and positive rotational speed, so there is no need for a bidirectional power electronics converter. The purely positive power also means that there is no need to raise the cut-in speed, so the wind turbine could harness power at all wind speeds. The trade-off is that the control rotor requires a high power rating. The power electronics require 260% of the power rating of the synchronous generator. This is undesirable because purpose of the control rotor is to merely support the power flow from wind turbine blades to the synchronous generator. Additionally, such a large power rating would result in a very costly drivetrain. For Case 1, the the maximum torque corresponds with the maximum speed, so there is no need for field weakening.

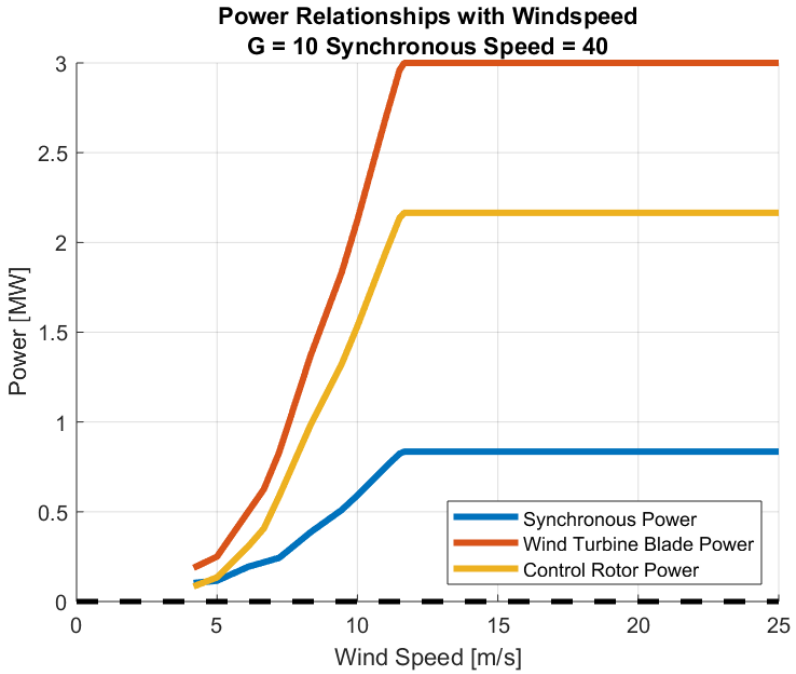


Figure 38. Power Relationship Curves for a Synchronous Speed of 40 rpm.

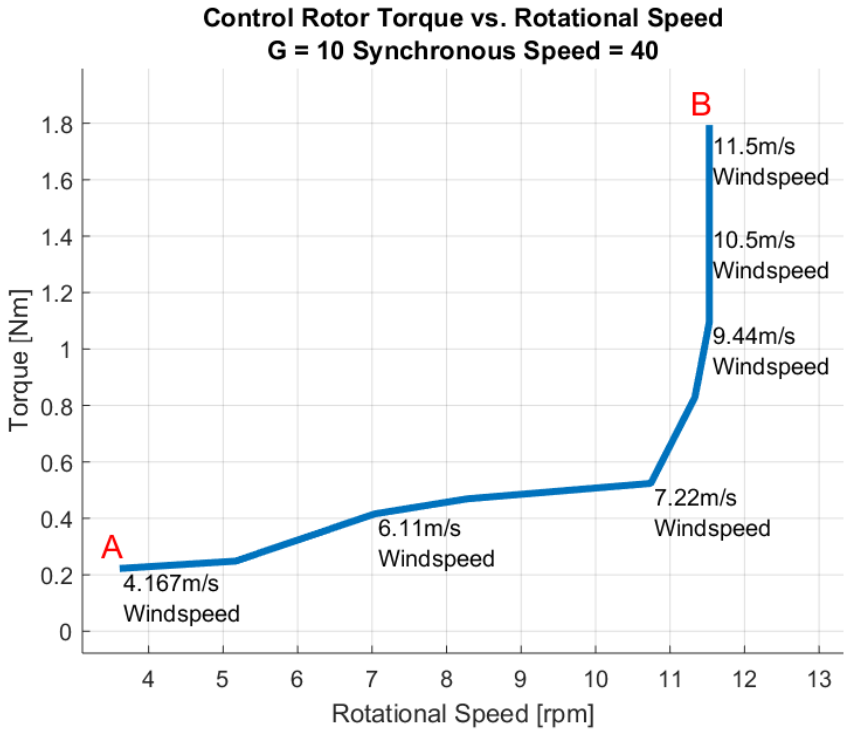


Figure 39. Torque vs. Rotational Speed for a Synchronous Speed of 40 rpm.

**Case 2**

Figures 40 and 41 show the Power Relationship plot and the Torque vs. Rotational Speed plot, respectively, for a synchronous generator speed of 80 rpm. Increasing the synchronous speed in Case 2 has decreased the power electronics power rating; however, it is still high at 80% of the power rating for the synchronous generator. Additionally, there is a small range of the windspeed that requires the control rotor to supply power to the system, requiring a bidirectional converter. Because the range of low windspeeds that require the bidirectional converter is so small, the unidirectional converter with a higher cut-in speed is a plausible solution that would not cause too much in the reduction of power. For this case, the cut-in speed is at 5 m/s, so areas that usually have windspeeds at or below that value would not be able to harness power. The high torque corresponds with the high torque in this case, so field weakening does not need to be considered.

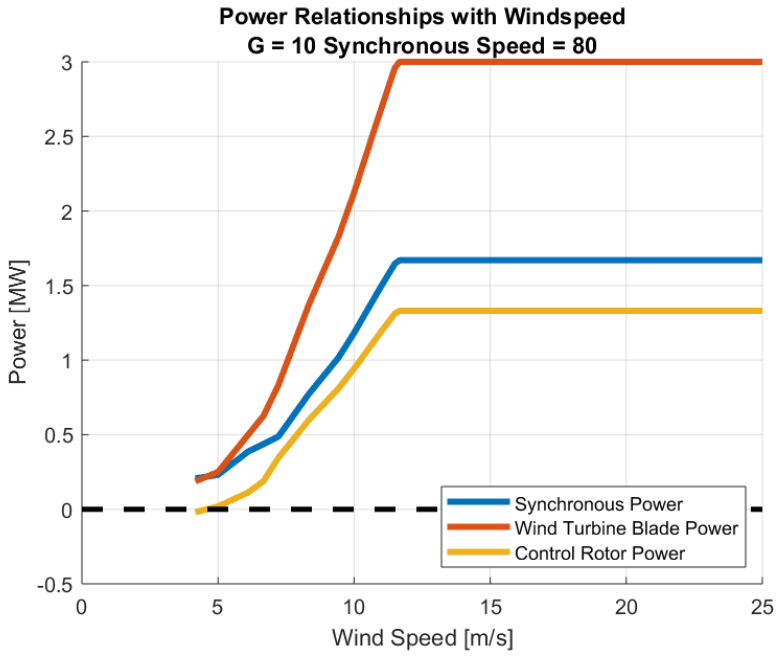


Figure 40. Power Relationship Curves for a Synchronous Speed of 80rpm.

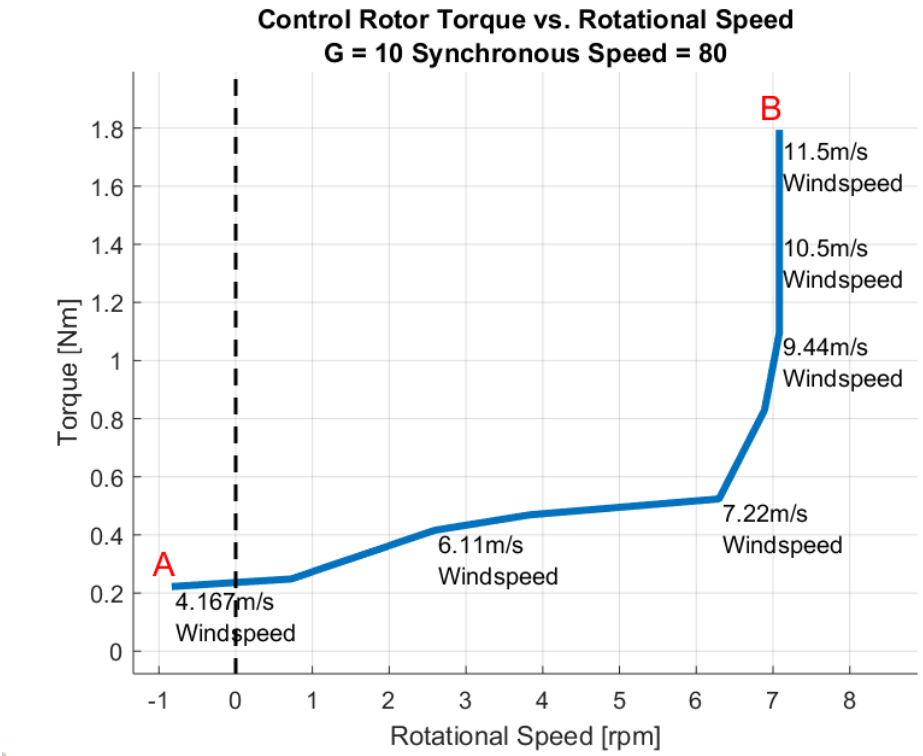


Figure 41. Torque vs. Rotational Speed for a Synchronous Speed of 80 rpm.

**Case 3**

Figures 42 and 43 show the Power Relationship plot and the Torque vs. Rotational Speed plot, respectively, for a synchronous generator speed of 120 rpm. Increasing the synchronous generator speed has again decreased the control rotor power rating; however, the decrease is much greater. In this case, the control rotor is only .5 MW and 20% of the synchronous generator power rating. This is a much more desirable power rating than the power ratings seen in Cases 1 and 2. There is also a growth in the range of windspeeds the power electronics must supply power. In order to have a unidirectional converter, the cut-in speed is now 7 m/s. This is still a relatively small cut-in windspeed, so just not harnessing power may be more beneficial than

paying for a bidirectional power electronics converter. In this case, the magnitude of the rotational speed required for the minimum torque is larger than the rotational speed required for the maximum torque, so field weakening is required. The speed ratio is relatively low at 2:1, which is in the range of most machine's capabilities to field weaken.

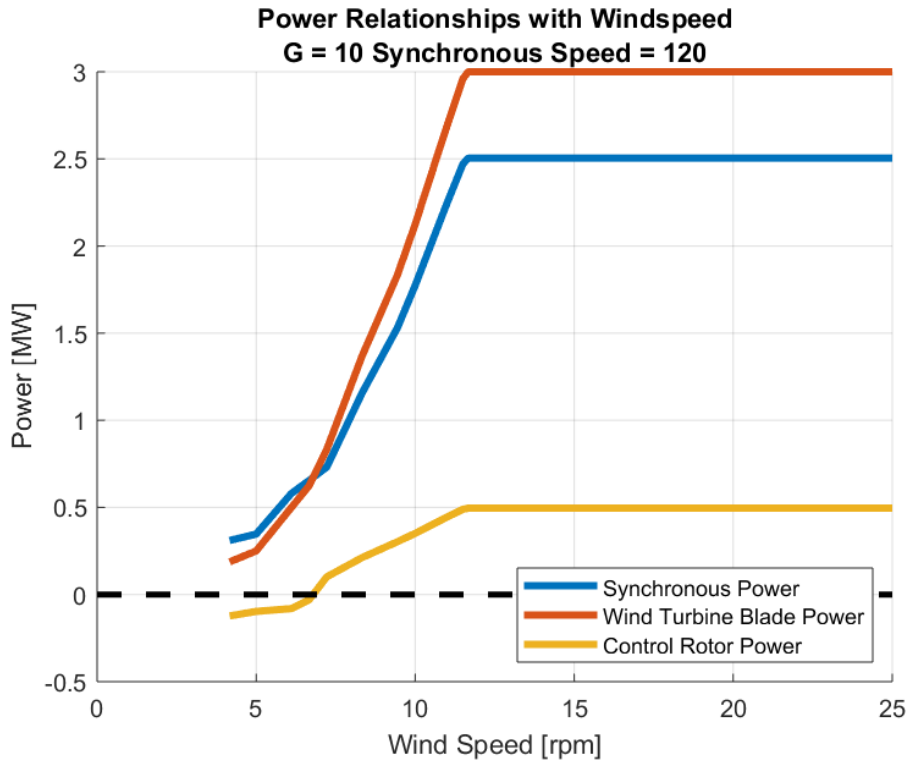


Figure 42. Power Relationship Curves for a Synchronous Speed of 120 rpm.

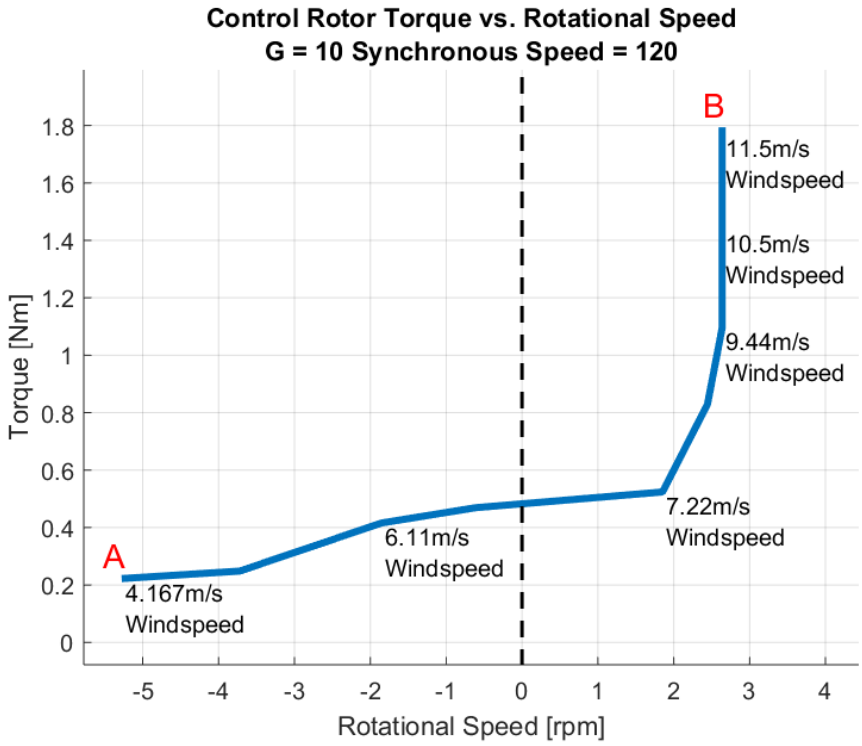


Figure 43. Torque vs. Rotational Speed for a Synchronous Speed of 120 rpm.

**Case 4**

Figures 44 and 45 show the Power Relationship plot and the Torque vs. Rotational Speed plot, respectively, for a synchronous generator speed of 145 rpm. In this case, the control rotor only takes power from the grid. This only calls for a unidirectional power electronics converter, but as shown in Figure 45, this requires also makes all of the rotational speed negative. The speed ratio for this case is especially high at 58:1. This is beyond most machines' capabilities to field weaken. Raising the cut-in speed would not create a significant difference because the high torque requires such a small rotational speed, the speed ratio will be greater than 10:1 until roughly windspeed of 7 m/s. This is not ideal because this makes the range of windspeeds where the wind turbine is not harnessing power large.

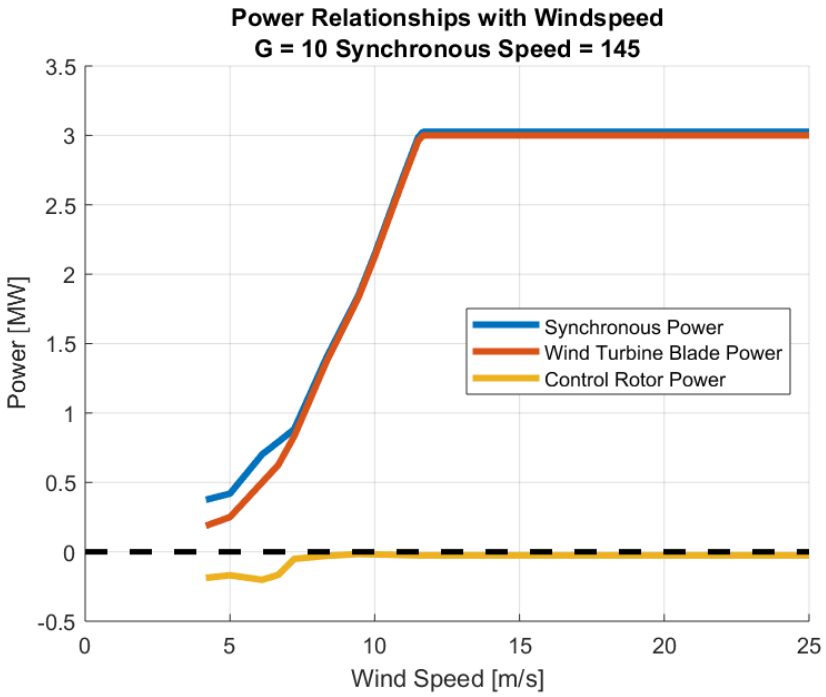


Figure 44. Power Relationship Curves for a Synchronous Speed of 145 rpm.

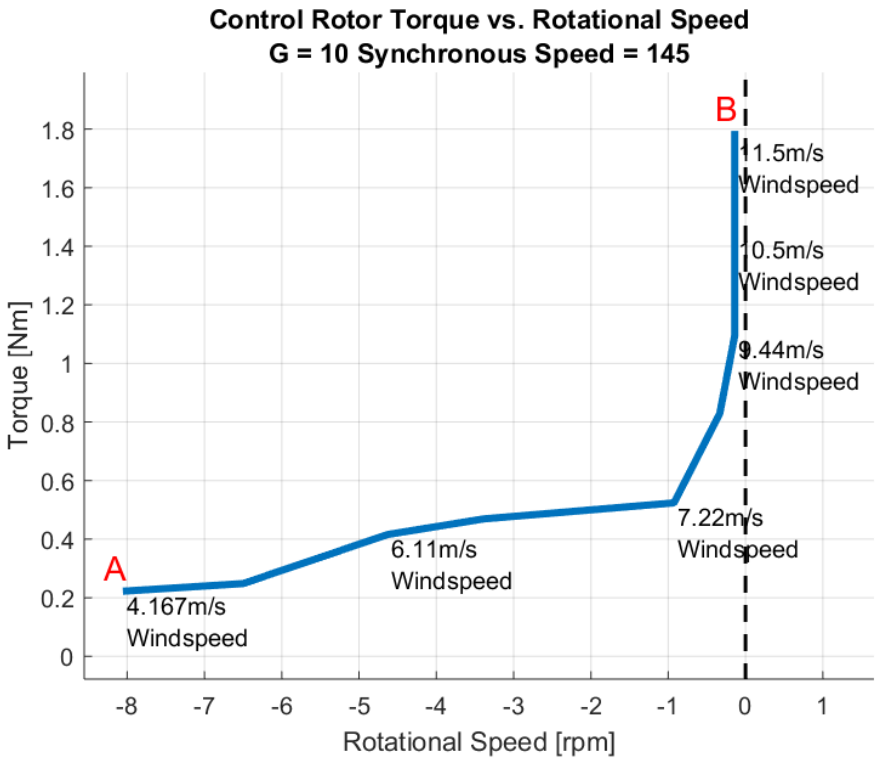


Figure 45. Torque vs. Rotational Speed for a Synchronous Speed of 145 rpm.

**Case 5**

Figures 46 and 47 show the Power Relationship plot and the Torque vs. Rotational Speed plot, respectively, for a synchronous generator speed of 160 rpm. In this case, Figure 46 shows that the control rotor only uses power. Because the power is only going in one direction, the power electronics only requires a unidirectional power converter. An undesirable effect is that Figure 47 shows that the Torque vs. Rotational Speed plot has moved entirely into the negative as well. This requires a negative voltage rating, and field weakening; however, neither are as severe as in Case 4. The speed ratio for this case is 5.37:1. This is still within most motors' field weakening capabilities. Because the control rotor is always using power and the amplitude is small, changing the cut-in speed is not a valuable solution. Changing the cut-in speed can change the speed ratio; however, the difference is not as significant because the entire plot is in the negative and the speed ratio is already within most machines' capabilities to field weaken.

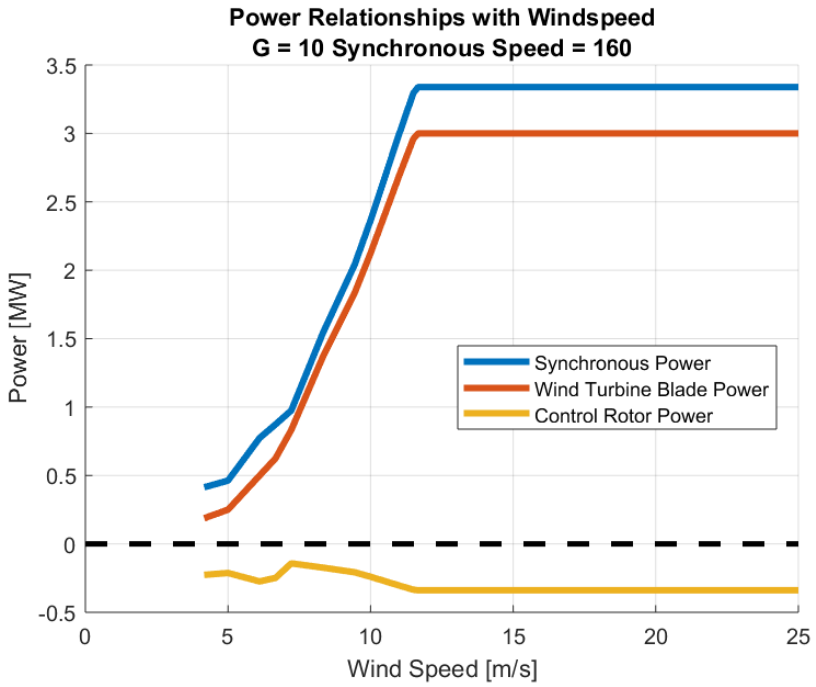


Figure 46. Power Relationship Curves for a Synchronous Speed of 160 rpm.

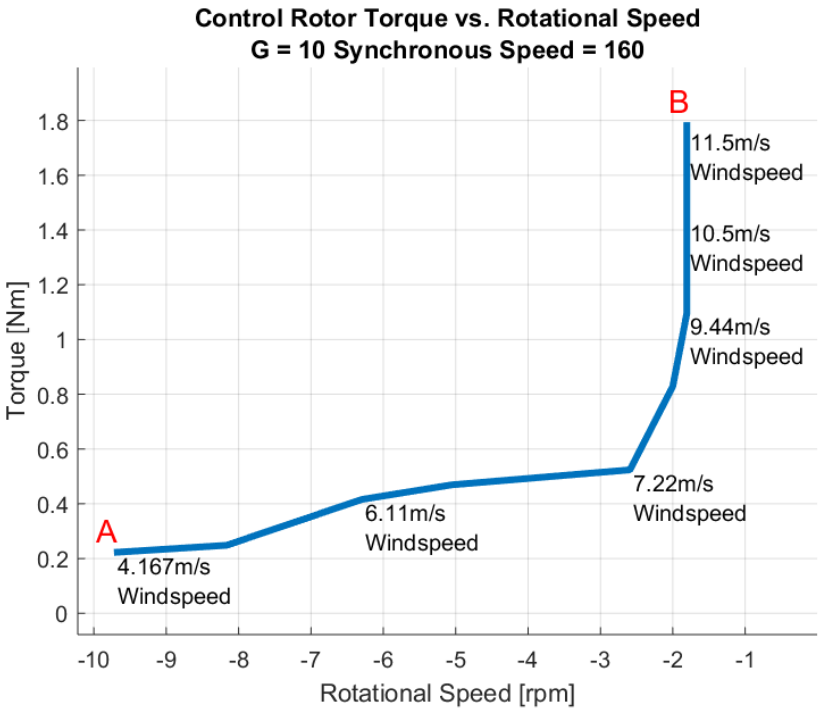


Figure 47. Torque vs. Rotational Speed for a Synchronous Speed of 160 rpm.

**Case 6**

Figures 48 and 49 show the Power Relationship plot and the Torque vs. Rotational Speed plot, respectively, for a synchronous generator speed of 200 rpm. The significant difference between Case 6 and Case 5 is that the maximum control rotor power has increased in magnitude. This makes it a greater percentage of the synchronous generator power which is undesirable. The Speed ratio has decreased from Case 5 to Case 6 to roughly 2:1 which is easily within most motors' field weakening capabilities. As in Case 6, changing the cut-in speed is not ideal because less power will be harnessed and there are not as many benefits. The control rotor uses power at all windspeeds, so it only needs a unidirectional power electronics converter, and the speed ratio is already within an easily field weakening range.

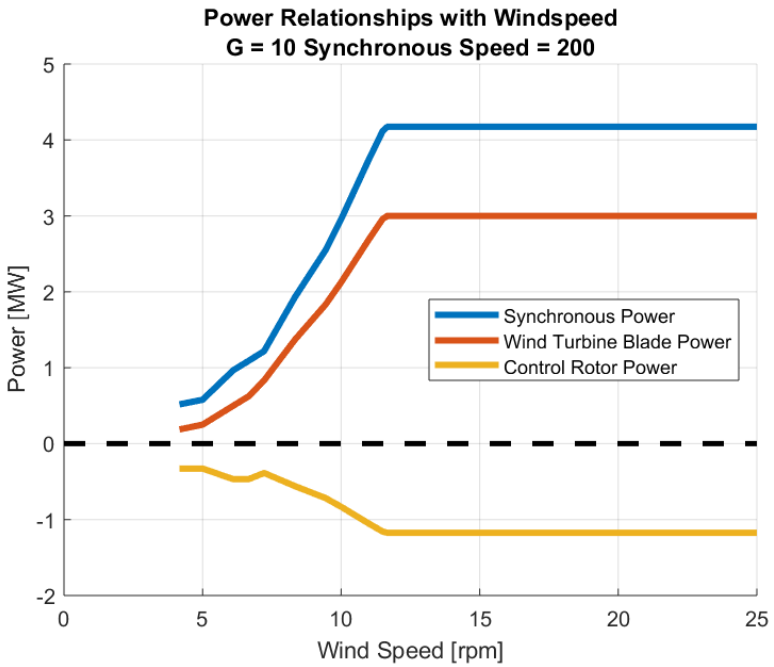


Figure 48. Power Relationship Curves for a Synchronous Speed of 200 rpm.

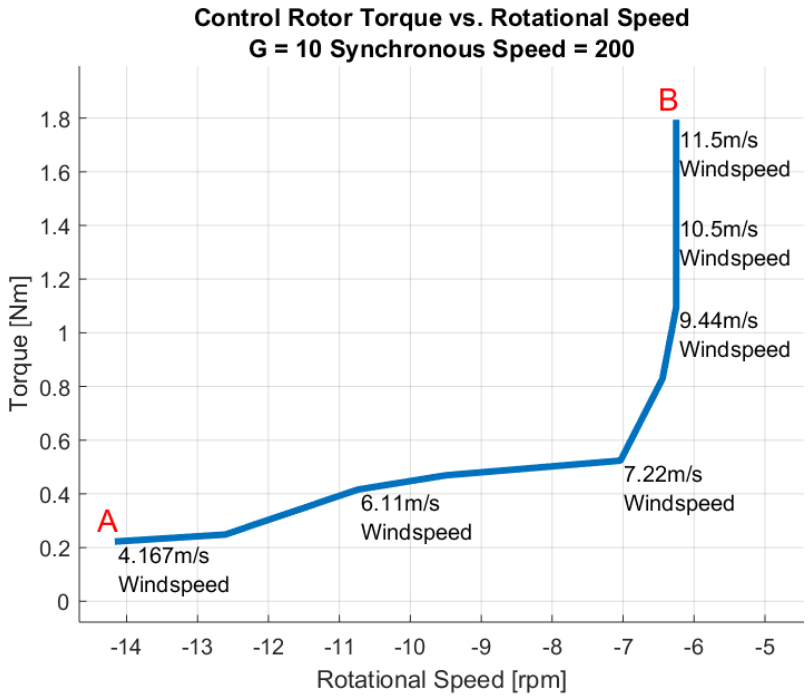


Figure 49. Torque vs. Rotational Speed for a Synchronous Speed of 200 rpm.

**Considering Gear Ratio**

In Cases 1-6, the gear ratio was fixed at 10, and only the synchronous generator rotational speed was changed. Figures 50 and 51 show the impact of changing the gear ratio on the speed ratio and the maximum power respectively. As shown in the two figures, the gear ratio value does not significantly change any of the scenarios. The possible power ratings and speed ratios are all still possible when the synchronous generator speed is changed over the same range. Therefore, the results in Cases 1-6 can be recreated with a different gear ratio using various synchronous generator speeds.

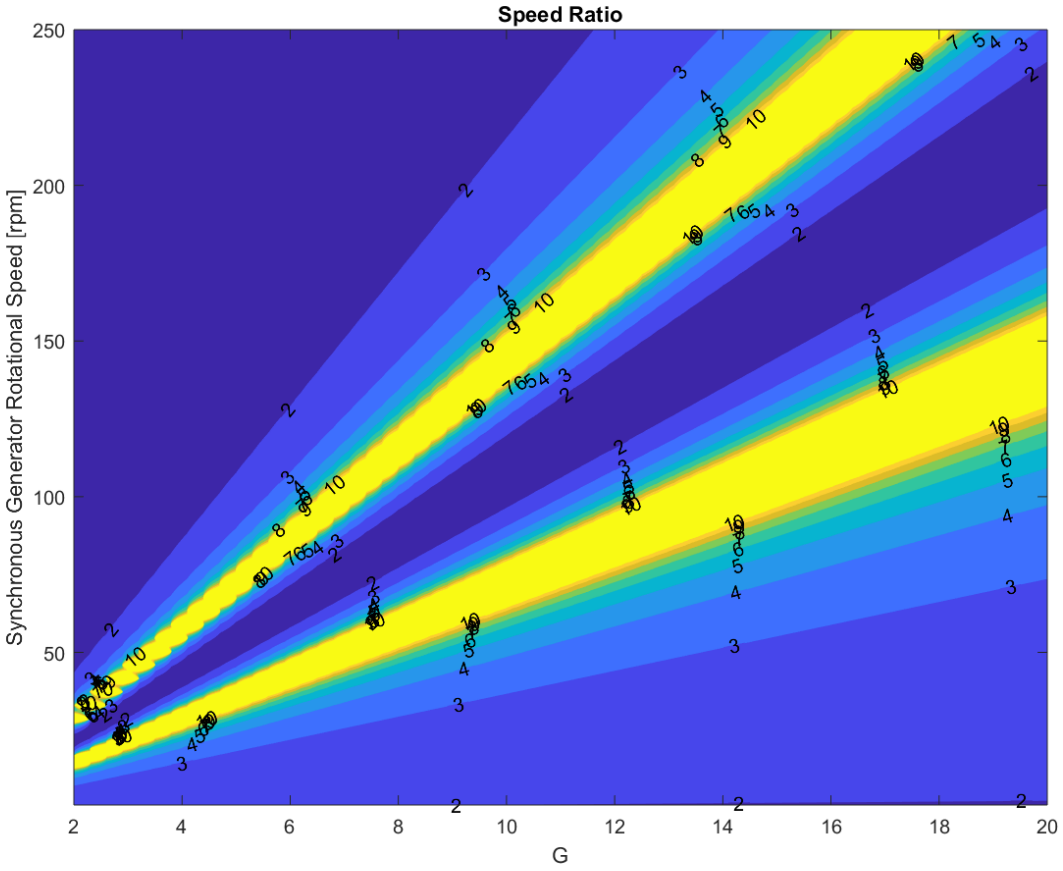


Figure 50. Gear Ratio and Synchronous Generator Speed Impact on Speed Ratio.

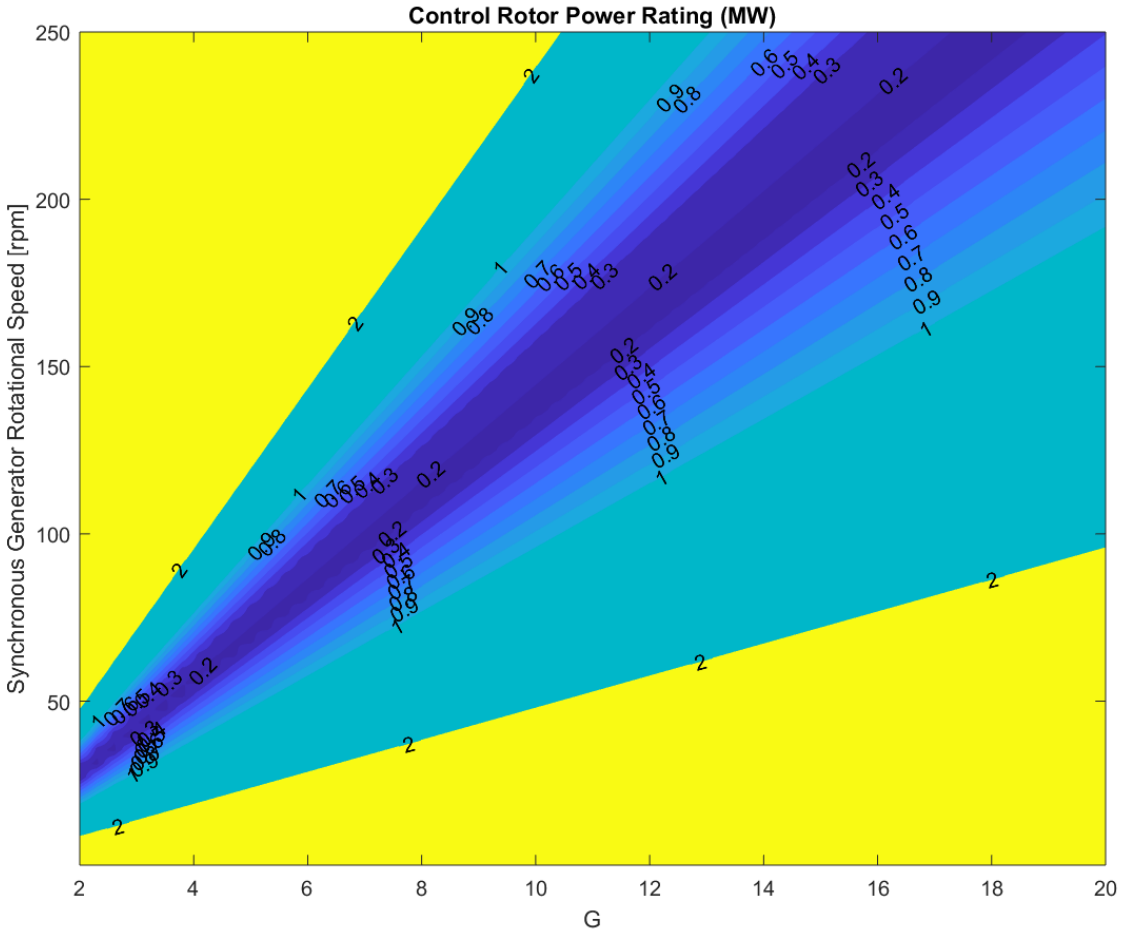


Figure 51. Gear Ratio and Synchronous Generator Speed Impact on Control Rotor Power Rating.

For both Figures 50 and 51, the ideal scenario is to minimize the speed ratio and the control rotor power rating. Minimizing the speed ratio, makes it easier to field weaken, and minimizing the control power rating decreases the cost and size of the power electronics required. In Figures 50 and 51, the optimum settings for the gear ratio and the synchronous generator are not the same for minimizing the speed ratio and minimizing the control rotor power rating. This means that there is a significant trade-off between the potential to field weaken and having a smaller power rating.

# CHAPTER VII

# CONCLUSION

This research presented a prototype and testbed to demonstrate the operation of a magnetic gear without contact. The prototype and testbed were used to test the impact of misalignment on the operation of magnetic gears. Several torque angle curves were created at various misalignments, and the deterioration of the curve and drop in peak torque were analyzed. The experimental data corroborated a lot of the simulation data; however, there were a few cases where the experimental data did not match. This is most likely attributed to imprecisions in measuring the misalignment and air gap on the testbed. Future iterations of this research will include a design that allows for a more precise measurement of the movement of the testbed. This data can be used to support future study in the benefits of magnetic gears over mechanical gears because of the less severe impact of misalignment to its operation.

Another contribution from this research is the study of drivetrain reduction for wind turbines using an mCVT. The impact of gear ratio and synchronous generator settings were observed on the operation of the control rotor and its power electronics. The relationship between the power rating of the control rotor and the synchronous generator speed and the relationship between the speed ratio and the synchronous generator speed was studied to determine the optimal settings and solutions for drivetrain reduction. From the simulations, it was found that the gear ratio does not have a great impact on drivetrain reduction because all of the speed ratios and power ratings can be achieved by changing the synchronous generator speed. It was found that there is a trade-off between trying to minimize the speed ratio and the power rating of the control rotor. Amongst the cases presented, it is shown that at a specified

gear ratio, a synchronous generator speed can be chosen to achieve a low control rotor speed to minimize the power rating and have a low cut-in speed. Case 3 showed the most promising configuration of the 6 cases because it has a low power rating which correlates with smaller and less expensive power electronics. In that case, the control rotor power is only negative, for a very small portion of the windspeed. Rather than using a bidirectional converter, raising the cut-in speed and using a unidirectional converter is a plausible solution. The unidirectional converter again decreases the size and cost of the power electronics in the drivetrain. Unless the area is only prone to low windspeeds below the cut-in speed, the wind turbines can continuously operate and harness power.

# REFERENCES


[1] Alkan, D. (2013). Investigating CVT as a Transmission System Option for Wind Turbines. [online] KTH School of Industrial Engineering and Management. Available at: https://pdfs.semanticscholar.org/d9ac/2a77c0111a52b14cffc756e8913034b7285c.pdf [Accessed 27 Jan. 2019].

[2] R.-J. Wang and S. Gerber, "Magnetically geared wind generator technologies: Opportunities and challenges," Applied Energy, vol. 136, pp. 817–826, 2014.

[3] P.M. Tlali, R-J. Wang, S. Gerber, "Magnetic Gear Technologies: A Review", International Conference on Electrical Machines (ICEM), 2014.

[4] Matthew Johnson, Matthew C. Gardner, Hamid A. Toliyat, "Design and Analysis of an Axial Flux Magnetically Geared Generator", IEEE Transactions on Industry Applications, Vol. 53, NO. 1, 2017.

[5] Matthew C. Gardner, Benjamin E. Jack, Hamid A. Toliyat, "Comparison of Surface Mounted Permanent Magnet Coaxial Radial Flux Magnetic Gears Independently Optimized for Volume, Cost, and Mass", IEEE Transactions on Industry Applications, Vol. 54, NO. 4, 2018.

[6] K. Atallah, J. Wang, "Design and Operation of a Magnetic Continuously Variable Transmission",IEEE Transactions on Industry Applications, Vol. 48, NO. 4, 2012.

[7] S.N. Udalov, A.G.Pristup, A. A. Achitaev, B. M. Bechenkov, Y.V. Pankratz, "Using a Magnetic Continuously Variable Transmission for Synchronization of Wind Turbine Generators Under a Variable Wind Speed", IEEE Dynamics of Systems, 2017.

[8] J.S. Hsu, "A Machine Approach for Field Weakening of Permanent-Magnet Motors", Society of Automotive Engineers, 1998.